Storm Surges

R.F. HENRY

Technical Report No. 19

Beaufort Sea Project

STORM SURGES

R.F. Henry

Institute of Ocean Sciences, Patricia Bay
Dept. of the Environment
1230 Government St.
Victoria, B.C. V8W 1Y4

Beaufort Sea Technical Report #19

Beaufort Sea Project
Dept. of the Environment
512 Federal Building
1230 Government St.
Victoria, B.C. V8W 1Y4

December, 1975

TABLE OF CONTENTS

1. SUMMARY

Storm surges, that is, storm induced increases in sea level, of about 1 m in amplitude and lasting for some hours are not uncommon on the Beaufort Sea coast in ice-free summers. Surge levels may even exceed 2 m in some embayments, for instance at Tuktoyaktuk. This report describes a study, involving numerical models, designed to permit prediction of surge levels between Herschel Island and Cape Bathurst and also to check if surge magnitudes at sites well off-shore are ever large enough to pose hazards to drilling operations.

At the coast, surges cause flooding and accelerated beach erosion and are a factor which should be considered in the design of artificial islands. The nesting sites of thousands of seabirds, of economic importance to the native population, can be inundated, and it is conceivable that the bird population might not survive contamination of the nesting grounds due to a surge carrying oil inland from a spill off-shore.

The accuracy of numerical storm surge models has to be verified by simulation of a number of actual surges. Too few surges have been successfully recorded in the Beaufort Sea to permit full quantitative model verification at the present time, but some confidence can be placed in the models in their present state, on account of experience with similar models of other seas. It can be concluded that storm surge amplitudes are much smaller at sites well off-shore than at the coast and are probably far less hazardous to drill-ships than other storm effects such as high winds and short-period waves. As more surge records accumulate, the models will be refined, but a limit to the accuracy of surge level forecasts is imposed by their dependence on forecast surface winds.

Two subsidiary topics discussed are 'negative surges', that is, temporary decreases in sea-level, which may hinder shipping, and winter surges, which though much less frequent than summer surges, should probably be considered during the design of near-shore structures, in view of their potential for causing ice damage.

2. INTRODUCTION

2.1 Scope of Study

Sea level elevations well above normal are experienced on the southern Beaufort Sea coast whenever strong northwesterly winds occur during the open-water season. Driftwood stranded 2 m or more above mean sea level indicates that the whole coast from Herschel Island to Cape Bathurst (Fig. 1) is affected by such storm surges. Recorded loss of life due to surges in this sparsely populated region has been low but the risk is increasing as oil and gas exploration intensifies. The principal aims of this study are to determine if surge levels in the off-shore areas where exploratory drilling is planned are comparable with levels reached near shore and to develop a forecasting system, based on numerical models, for prediction of expected surge levels over the whole Mackenzie-Bathurst shelf.

Storm surges have important implications in several other studies in the Beaufort Sea Project. A major surge can flood huge areas of the

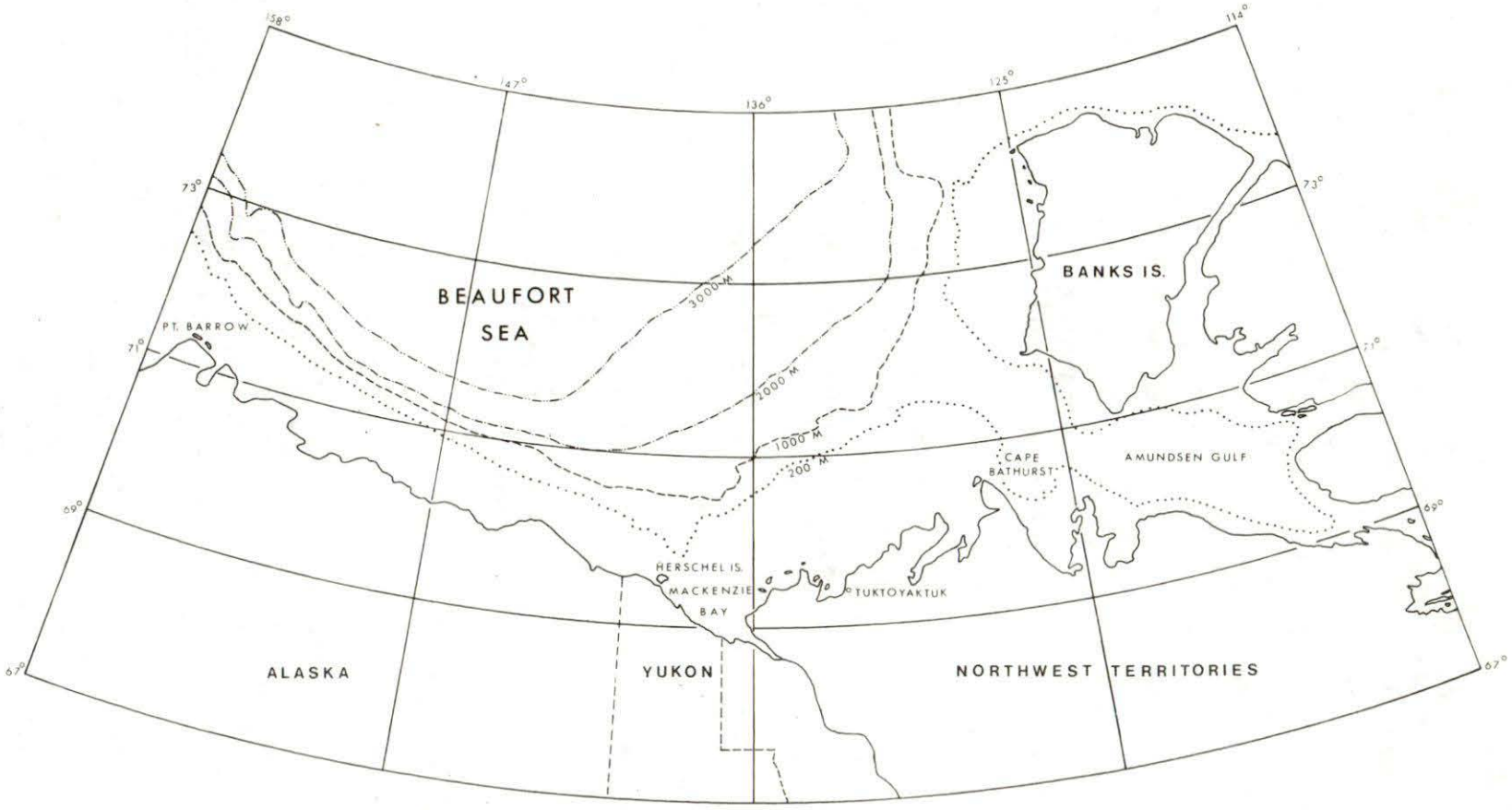
158°
147°
136°
125°
114°
73°
71°
69°
67°
BEAUFORT SEA
BANKS IS.
PT. BARROW
3000 M
2000 M
1000 M
200 M
CAPE BATHURST
AMUNDSEN GULF
HERSCHEL IS.
MACKENZIE BAY
TUKTOYAKTUK
ALASKA
YUKON
NORTHWEST TERRITORIES

Figure 1

low-lying coastal lands between Mackenzie Bay and Cape Bathurst. Many thousands of seabirds, of economic importance to the native population, nest in this area in the summer months when storm surges are most likely to occur. The combined effects on these of an oil spill and storm surge would probably be disastrous. Most of the coastline is subject to fairly rapid erosion. Storm surges greatly accelerate this process and at some points the retreat of the shoreline during a major surge - as much as 20 m - is equivalent to several normal years' erosion.

2.2 Storm Surge Forecasts

The storm surge study is one of several intended to permit *prediction* of weather and sea conditions up to 36 hours in advance. Forecasts of dangerous water levels, winds, wave conditions and ice movements can improve the efficiency of marine operations such as exploratory drilling from ships. It is desirable to have warning of when to disconnect equipment from the sea bottom. Even a few unnecessary shutdowns could waste a substantial portion of the short drilling season, so that accuracy of prediction is highly desirable. Other applications of water level forecasts would be to alert investigators of wildlife and beach morphology to conditions of interest, or in extreme cases to permit evacuation of personnel from low-lying camps. Negative surges in which the sea level falls as much as 1 m below normal are not uncommon on the shelf during periods of strong off-shore winds. The approaches to Tuktoyaktuk, the only harbour in the area, have a draft of only 4 m and accurate prediction of significant reductions is important for supply shipping.

The need for predictive capability is being met by development of related meteorological and oceanographic models of which those relevant to storm surges are described in this report. These will be run hourly to assist in the preparation of 36-hour comprehensive environmental forecasts issued by Arctic Weather Central, Edmonton, the responsible regional office of the Atmospheric Environment Service of Environment Canada. The reliability of water level forecasts will depend on the accuracy of the predicted winds obtained from the meteorological models and on knowledge of the extent of open water, about which information can be obtained at present only some days in arrears from satellite photographs.

2.3 Available Data

Verifying oceanographic models and checking the accuracy of subsequent surge predictions requires synoptic records of a reasonable number of actual surges. Prior to the Beaufort Sea Project, only once (September 1-2, 1972) did a surge occur when more than one water level gauge was in operation. An extensive field program of coastal and off-shore gauging was mounted in the summer of 1974 but no surges occurred because of unusually persistent ice cover, which also prevented the recovery of off-shore instruments. The field program was repeated in 1975; this was a much more favourable year and synoptic records of two surges of approximately 1 m were recorded in August. Processing of the water level and meteorological records prior to numerical simulation runs is still in progress.

Fairly complete water level records taken at Tuktoyaktuk for twelve winters prior to 1973/74 show no significant surge activity but positive surges of approximately 1 m were recorded on gauges at Herschel Island, at Tuktoyaktuk and at an off-shore site during the passage of intense cyclonic systems on November 11-14, 1973 and January 1-7, 1974. Ice cover was practically total on those occasions, but the slight movement still possible in the ice cover apparently permitted transmission of momentum to the water via tangential wind stress. Inclusion of ice cover in a numerical model would require information about the extent of shorefast ice and the freedom of movement remaining in the pack ice beyond, neither of which can be determined yet by remote sensing techniques. Consequently, the numerical oceanographic models do not include the dynamics or the effects of ice cover and the winter surge records unfortunately cannot be used yet for model verification.

3. PHYSICAL FEATURES OF THE SOUTHERN BEAUFORT SEA RELEVANT TO STORM SURGES

3.1 Bathymetry

Proposed oil exploration is limited to a wide shallow shelf which extends from Herschel Island at the western limit of Mackenzie Bay to Cape Bathurst, approximately 400 km to the east (Fig. 1). Water depth increases very gradually with distance northward to about 100 m at the edge of the shelf roughly 140 km from the coast. The only exceptional feature is the Herschel Canyon which extends southward from deep water northeast of Herschel Island towards the mouth of the Mackenzie River. North of the shelf the sea bottom slopes down relatively quickly to depths of more than 3000 m, typical of the central Beaufort Sea. On the eastern edge of the shelf, there is a similar abrupt drop to the lesser depths of the Amundsen Gulf. In the west, a narrow shallow connection around Herschel Island to the Alaskan shelf may permit transmission of long waves travelling eastward with storm systems, but otherwise the Mackenzie-Bathurst shelf can be considered as an isolated shallow-water system bordered on its open boundaries by much deeper water.

East of the international boundary at 141°W the deep water for some distance north of the shelf has been sounded recently through the ice by the Polar Continental Shelf Project of the Department of Energy, Mines and Resources, while the Canadian Hydrographic Service has surveyed the shelf itself by conventional means. With the exception of eastern portions of Amundsen Gulf and the deep water west of the international boundary, bathymetric information about the Mackenzie-Bathurst shelf and its environs is adequate for storm surge studies.

3.2 Coastal Topography

Almost all the coastal land from Mackenzie Bay to Cape Dalhousie at the eastern tip of the Tuktoyaktuk Peninsula stands barely above sea level, even for considerable distances inland. During major storm surges, it forms a large flood plain more than 1000 km^2 in extent. For accurate forecasting of maximum surge elevations, it is necessary to simulate flooding of the coastal plain. Quantitative evidence of the extent of flooding during past surges is lacking, but neverthe-

less, reasonably accurate simulation should be possible once accurate topographical information becomes available. No overall geodetic levelling has been carried out and terrain heights have been measured with respect to local mean sea level. As it is now known that this datum varies substantially from season to season, depending on the extent of ice-cover in the southern Beaufort Sea (§3.3), a thorough review of the available topographic information is required.

Accelerated erosion during storm surges is a major factor in the small-scale geomorphology of the Beaufort Sea coast (Ref. 1). The cliffs along the Yukon coast on the west of Mackenzie Bay consist of frozen sediment which is rapidly undercut by wave action during surges. While the rate of coastal retreat is dramatic by geological standards, it is measured in metres per year at most and so is completely negligible as far as storm surge modelling is concerned.

3.3 Stratification

Flow in the Mackenzie River increases rapidly in May each year, reaching a maximum of around 17000 - 22500 m^3/s in June and then decreasing steadily to winter levels of 2000 - 3000 m^3/s by December. This fresh water discharges into the Beaufort Sea in undetermined proportions through the many channels of the Mackenzie Delta. Salinity measurements indicate that a low salinity surface layer is established in the summer months, with a sharp halocline varying in depth from 2 to 4 m in years when there is extensive open water (Ref. 2) to as much as 10 m in bad ice years (Ref. 3). The steric change in sea level due to a change of 8 m in halocline depth would be approximately 0.2 m, assuming a difference of 25.0 in σ_t between the two layers. In fact, increases of about 0.3 m in level have occurred in bad ice years such as 1964 and 1974, so it appears that the damming in of the fresh water by the ice produces a dynamic as well as a static contribution to the change in sea level.

Both satellite and surface observations indicate that the low-density layer forms a generally eastward moving plume with a sharply-defined northern boundary which can move rapidly over large distances as the surface wind varies. Numerical models of two-layer situations such as this require a good deal more computing capacity than the single layer models developed in this study and could not be run on the computer installation to be used for operational forecasting. So far as is known, stratification does not significantly affect storm surges.

3.4 Ice Cover

Since 1962 the extent of ice cover has been recorded by trained observers on regular flights made over the southern Beaufort Sea during the daylight months. The geographical extent of the ice cover is highly variable from year to year and even from day to day, especially at the beginning and end of summer. In some summers, the southern edge of the pack ice may retreat so far northwards that for storm surge forecasting purposes the whole sea can be considered ice-free (Figure 2). The 'fetch' or distance over which momentum can be transferred from the wind to the sea is then limited only by the scale of the weather systems and large surges can arise if severe

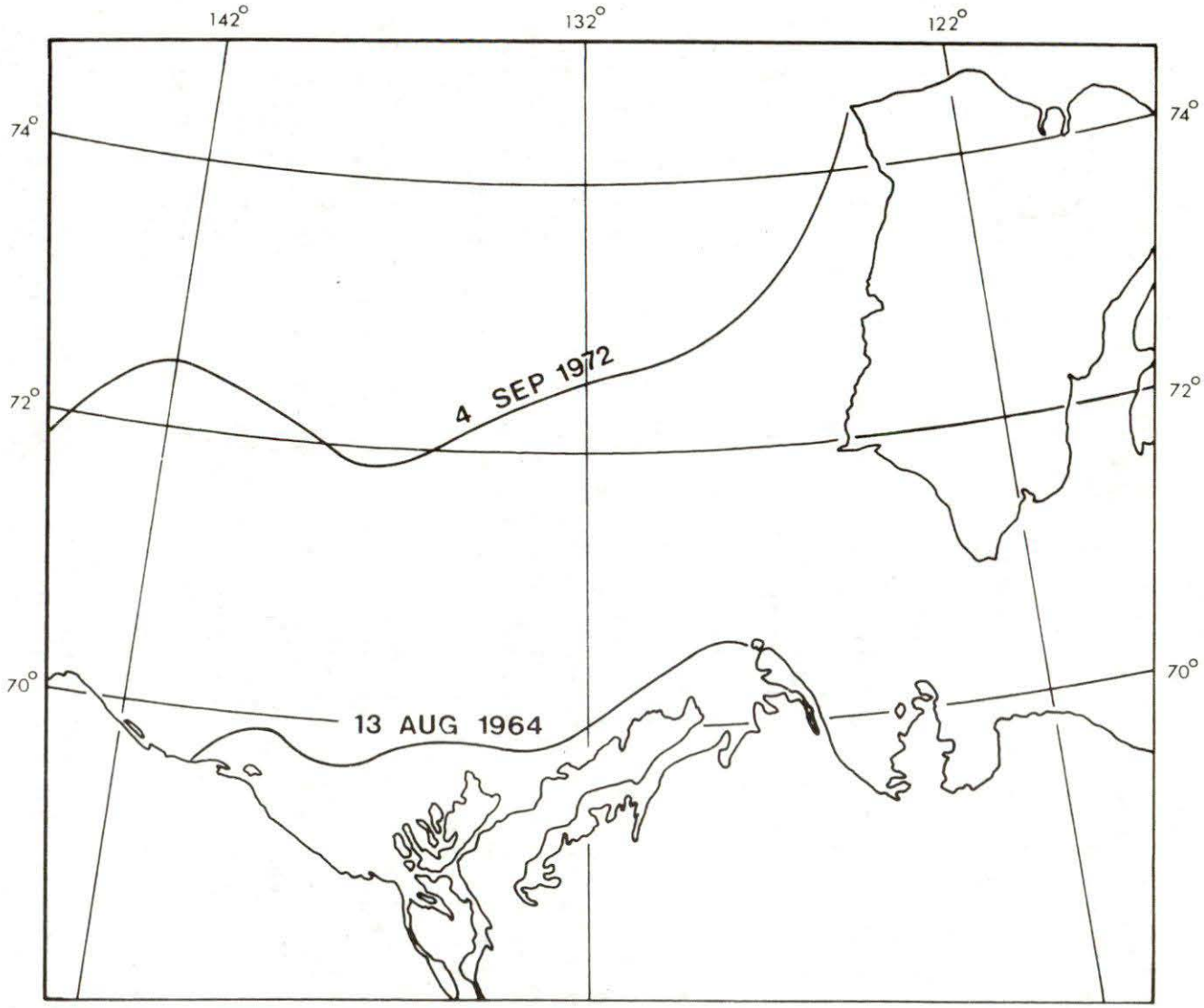

Northern Limit of Open Water

Figure 2

storms occur. In bad ice years, on the other hand, the ice may remain within tens of kilometres of the coast all summer, severely curtailing the wind fetch and thus limiting surge activity. Though it is clear that surface winds have major influence on ice movement, the combination of factors which governs the extent of ice cover is poorly understood at present and for this reason it is not possible to give long-range forecasts of surge likelihood.

When ice cover is present, its nature and degree varies very considerably, from 10/10 unnavigable pack ice in the central Beaufort Sea to practically open water dotted with isolated floes, typical of summer breakup. From the point of view of storm surge generation, minor amounts of ice cover, perhaps up to 2/10 or 3/10, where there is low probability of floes conglomerating, may be effectively equivalent to open water, but in fact nothing quantitative is known about meso-scale wind stress in the presence of partial or total ice cover. The role of ice cover during winter surges is discussed in §7.

3.5 Meteorology

The climatology of the Beaufort Sea has been reviewed recently in detail by Burns (Ref. 4). In winter, the dominant circulation over the southern Beaufort Sea is anticyclonic, with primary and secondary highs travelling roughly northwest to southeast. Some secondary lows pass eastwards about the latitude of northern Banks Island or further north and two winter surges discussed later were caused by storms of this type. In spring, as the days lengthen and the solar energy input increases, some instability develops in the air mass and penetration of frontal lows becomes more frequent. Cyclonic activity is maximum in July and August.

Upper air flow weakens in summer and becomes more westerly. In general, primary lows follow inland southwesterly or westerly corridors but in the late summer secondary lows tend to follow a west-east corridor centred about 70°N, that is, along the southern Beaufort Sea coast. It is these systems which, in ice-free years, cause positive storm surges.

The shortness of the meteorological record, about twenty years, prevents any reliable estimation of extreme winds, though it does permit broad statements about ordinary conditions. The negligible number of observations made in the area from ships has limited the sources of information to observations made at shore stations, some of which are heavily modified by local topography, and to estimates made using large-scale numerical atmospheric models. Burns warns that particularly in the presence of a surface cold front, winds over the water may be two to four times stronger than those reported along the coast. Recent efforts at meso-scale modelling to improve estimates of surface winds are discussed in § 6.

4. WATER LEVEL OBSERVATIONS ON THE MACKENZIE-BATHURST SHELF

4.1 Tide Gauge Records at Tuktoyaktuk

The first storm surge of which any account survives occurred early in September, 1944, when the combined effects of surge, tide and shorter period waves may have exceeded 3 m at Tuktoyaktuk (Ref. 5). Recording of water levels began with the installation by the Canadian Hydrographic Service of a permanent tide gauge at Tuktoyaktuk in 1962. Gaps have occurred in the records due to difficult operating conditions, but substantially complete records have been obtained in various years. Among these are 1962 and 1963, which had large areas of open water - conducive to surge activity - during the summer months and, near the other extreme, 1964 and 1974 which had summers with unusually persistent ice cover. It is regrettable that the Tuktoyaktuk gauge was not in operation during the destructive surge of September 13-16, 1970, which appears to have been the most severe since 1944 (Ref. 5), nor in September 1972 when another more modest surge was recorded on four temporary gauges at Pelly Island, Atkinson Point, Cape Dalhousie and Cape Bathurst.

The Tuktoyaktuk records serve at least to indicate the variability in surge occurrence. Figure 3 shows daily extrema of water levels at Tuktoyaktuk for 1962-64 and 1974. Positive extrema less than 1 m and negative extrema less than 0.5 m in magnitude have been omitted. A seasonal distribution of positive and negative surge activity is evident. Negative surges occur irrespective of the degree of ice cover, but the suppression of positive surges by the persistent ice-cover in 1964 and 1974 is clear. The apparently anomalous positive winter surge in January 1974 is discussed in § 7.

The maximum tidal range attributable to diurnal and higher frequency constituents at Tuktoyaktuk is approximately 0.37 m and Figure 3 would not be essentially altered if this tidal contribution were removed. The tidal ranges measured at other temporary stations on the Mackenzie-Bathurst shelf are comparable with that at Tuktoyaktuk. Since tidal amplitudes are small relative to those of major surges, it is reasonable to assume that the tide has little effect on surge amplitude. Consequently, it is assumed in this phase of the study that estimates of extrema in water level may be obtained by addition of computed surge elevation and predicted tide. Precise prediction of the times at which extrema occur would obviously require detailed observation and simulation of the changes in tidal phase which occur during surges.

Analyses of the Tuktoyaktuk records show considerable variation in tidal constituents slower than diurnal and it is probable that meteorological effects completely mask any true tidal effects in this frequency range. Analysis is complicated by the fact that on a monthly or seasonal scale there is some variation in mean level which is not of tidal or meteorological origin. In 1964 and 1974, the persistent ice cover apparently hemmed in the fresh water discharged in summer from the Mackenzie River, resulting in a temporary increase in mean level of roughly 0.3 m from June to September. However, in ice-free summers such as 1962 and 1963 this effect was not noticeable.

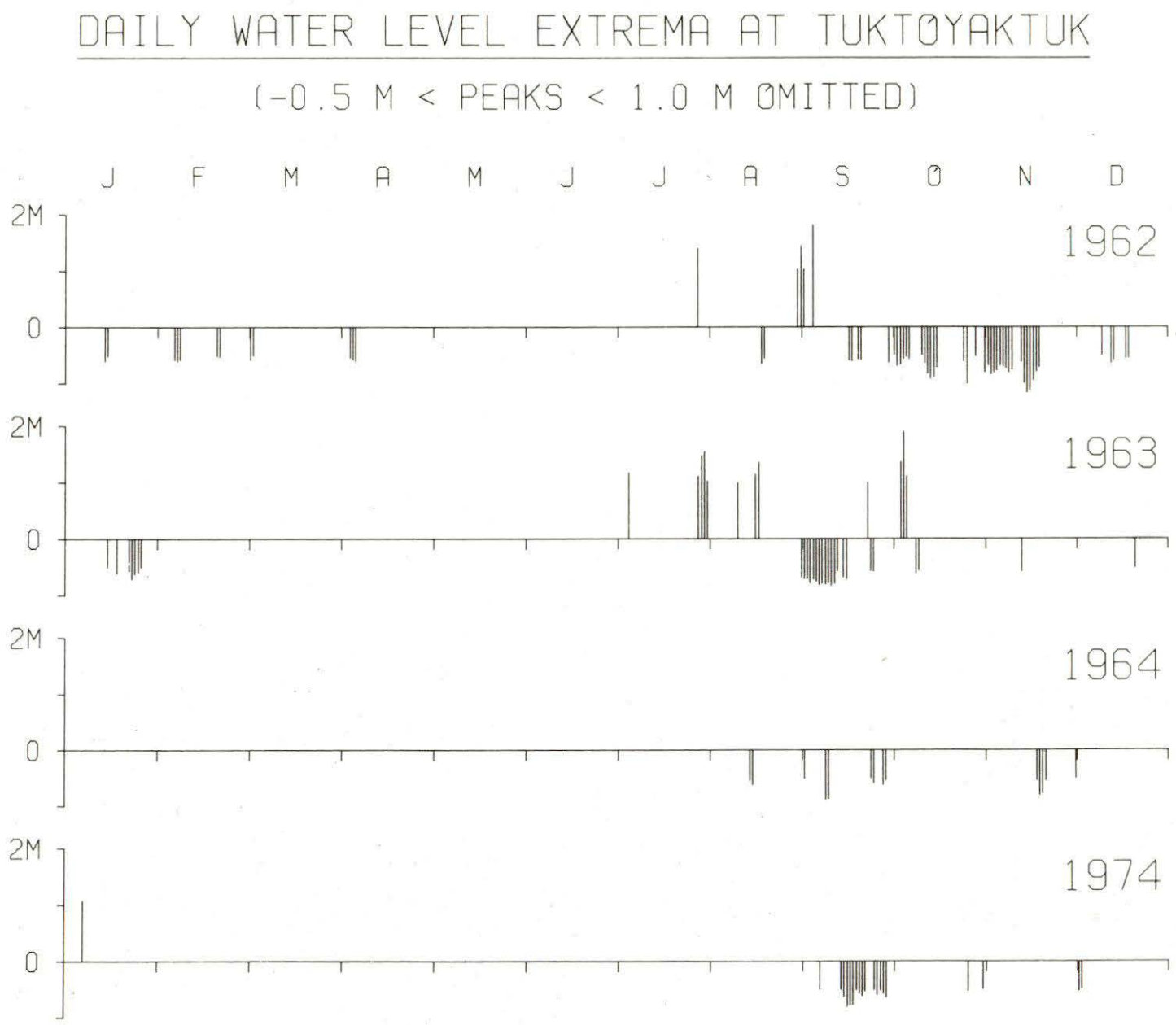
DAILY WATER LEVEL EXTREMA AT TUKTOYAKTUK
(-0.5 M < PEAKS < 1.0 M OMITTED)
J F M A M J J A S O N D
2M
0
1962
1963
1964
1974

Figure 3

Mean sea level calculated on an annual basis has been constant at Tuktoyaktuk since gauging began in 1962.

4.2 Synoptic Observations of Surges

On September 2, 1972, during the eastward passage of a low pressure system across the southern Beaufort Sea (Figure 4) partially synoptic coverage of a positive surge of about 1 m was obtained from temporary tide gauges at Pelly Island, Atkinson Point, Cape Dalhousie and Cape Bathurst (Figs. 5 and 6). Some useful checks of surge simulation and prediction techniques have been carried out using the September 1972 records. This surge, though smaller in magnitude, resembled the major 1944 and 1970 surges in that it occurred during strong north-west onshore winds.

In order to verify numerical models adequately, it is of course necessary to have a substantially wider variety of synoptically recorded surges to simulate. With this in mind, an extensive network of water level gauges and current meters was deployed in early 1974 during the first field season of the Beaufort Sea Project (Fig. 7). These instruments were installed through holes blasted in the ice by helicopter-borne parties, but none of the off-shore instruments could be recovered in the fall of 1974 due to the persistent ice-cover. An almost identical layout of gauges was deployed again in the spring of 1975. During the summer the extent of open water was much greater than at any time in 1974 and most of the instruments were recovered. Two off-shore gauges (Sites 5 and 13, Figure 7) and eight shore-based gauges were still in operation when surges of about 1 m occurred on August 10-11 and August 27, 1975. When processing of these records and the contemporary meteorological data is complete, there will be practically enough data to verify model predictions of surges of moderate amplitude. Subsequent extrapolation to larger amplitudes is questionable and verification of the models for surges such as those of 1944 and 1970, which went unrecorded, must await the recurrence and successful recording of similar exceptionally large surges.

In the fall of 1973, a bottom-mounted off-shore tide gauge was installed at Site 13 in 35 m of water 100 km NNW of Tuktoyaktuk. The gauge operated successfully throughout the 1973/74 winter, as did two shore-based gauges at Herschel Island and Tuktoyaktuk. All three gauges recorded positive surges roughly 1 m in magnitude on November 12, 1973 and January 9, 1974, at which times ice cover in the area was practically complete. The numerical models developed so far are intended for the ice-free summer period. Consequently, the partially synoptic winter surge records just described cannot be used to verify numerical models, until the latter are modified to include ice cover, as discussed in § 7.

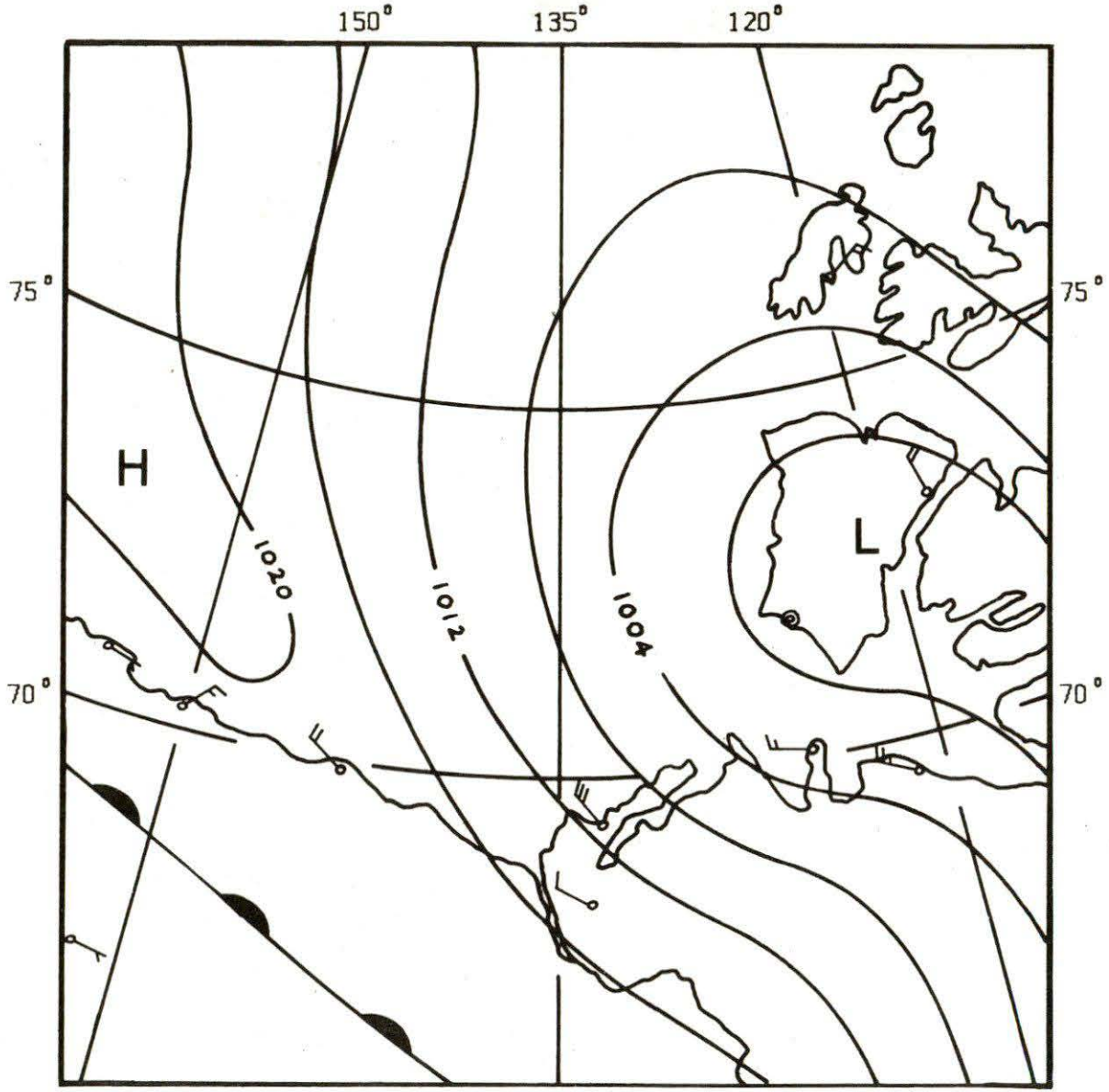
150°
135°
120°
75°
75°
70°
70°
H
L
1020
1012
1004
SURFACE PRESSURE (MB) AT 0600 GMT 2 SEP 1972

Figure 4

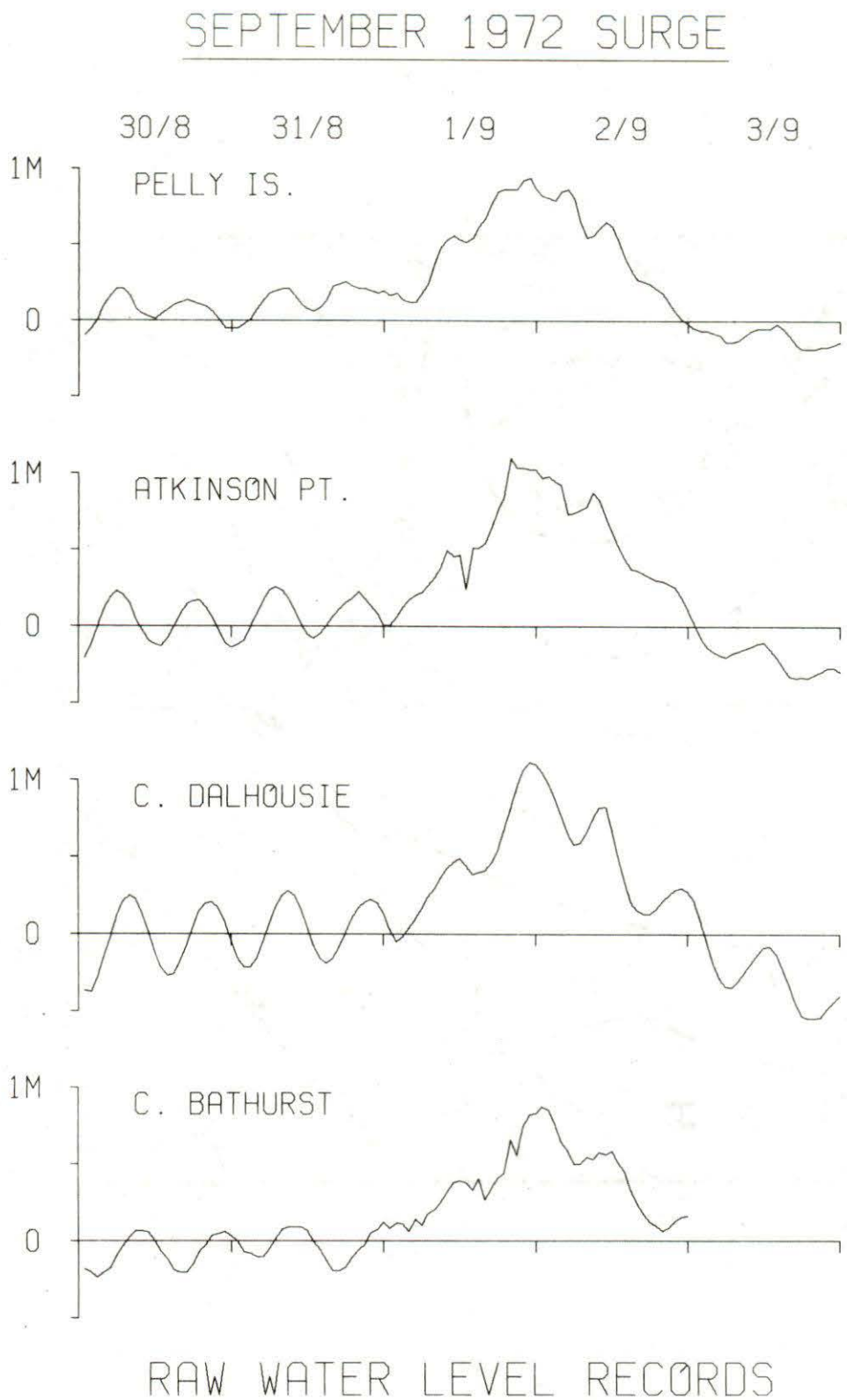
SEPTEMBER 1972 SURGE
30/8
31/8
1/9
2/9
3/9
1M
PELLY IS.
0
1M
ATKINSON PT.
0
1M
C. DALHOUSIE
0
1M
C. BATHURST
0
RAW WATER LEVEL RECORDS

Figure 5

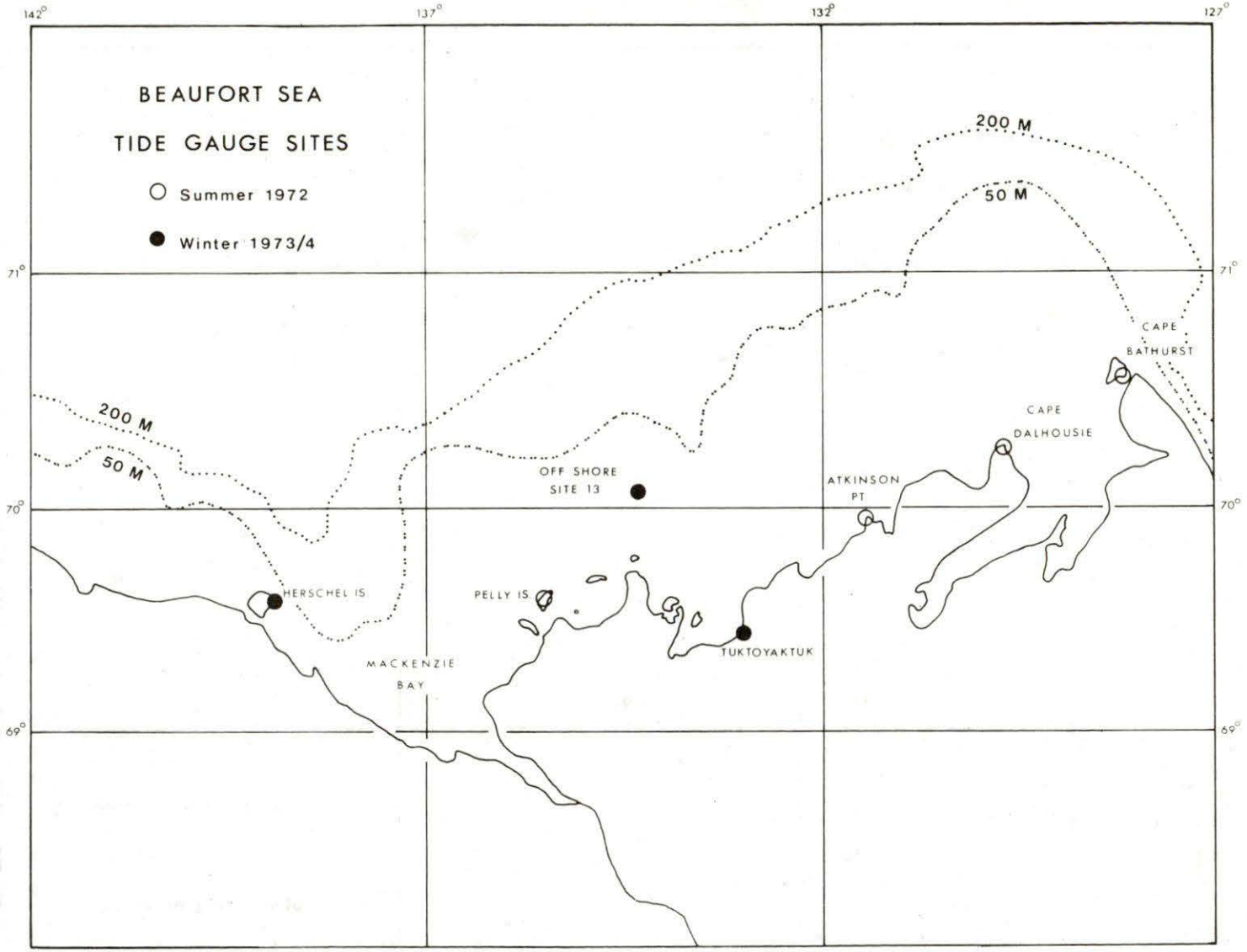
BEAUFORT SEA
TIDE GAUGE SITES
Summer 1972
Winter 1973/4
142°
137°
132°
127°
71°
70°
69°
200 M
50 M
200 M
50 M
CAPE
BATHURST
CAPE
DALHOUSIE
ATKINSON
PT
OFF SHORE
SITE 13
HERSCHEL IS
PELLY IS
TUKTOYAKTUK
MACKENZIE
BAY

Figure 6

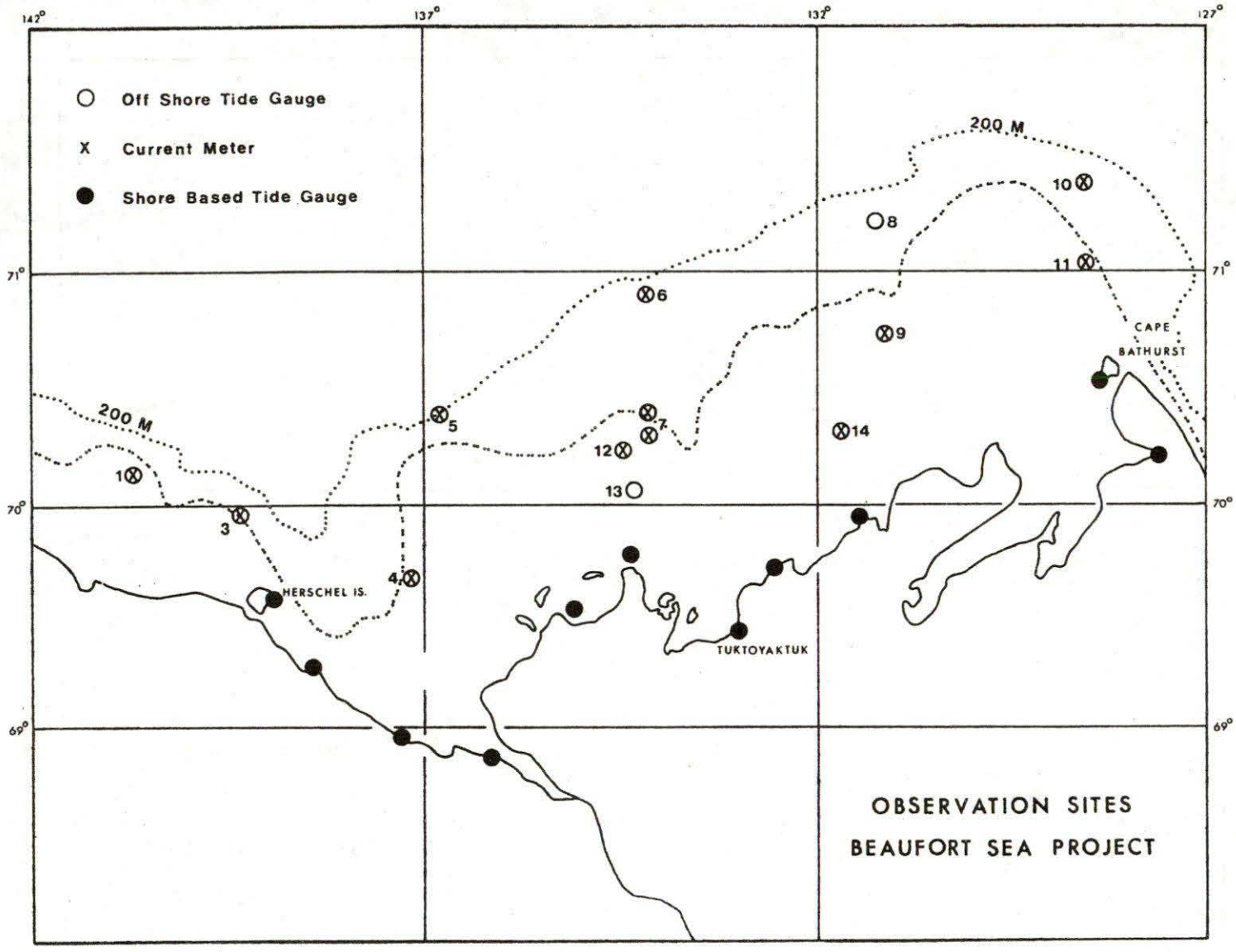
142°
137°
132°
127°
71°
70°
69°
Off Shore Tide Gauge
Current Meter
Shore Based Tide Gauge
200 M
200 M
1
3
4
5
6
7
8
9
10
11
12
13
14
HERSCHEL IS.
TUKTOYAKTUK
CAPE BATHURST
OBSERVATION SITES
BEAUFORT SEA PROJECT

Figure 7

5. NUMERICAL STORM SURGE MODELS

5.1 The Large-Area Model

Two one-layer numerical models have been developed in the course of this study. One of these, which will be referred to as the large-area model, stretches from 116°30'W to 156°30'W and from 68°30'N to 74°N (Figure 8), thus including practically all areas of the Beaufort Sea known to have been ice-free on any occasion. Spherical polar co-ordinates are used in view of the large latitudinal range. The grid intervals are one sixth of a degree of latitude and one half of a degree of longitude; grid interval length in the centre of the model is thus about 18 km. Shallow Bay, the diverging westernmost mouth of the Mackenzie River, and the inlet known as Eskimo Lakes, parallel to the Tuktoyaktuk Peninsula are simulated by one-dimensional appendages to the main two-dimensional model. The number of grid-points involved is much too high for the large-area model to be run on the computer available for hourly forecasting and the cost of running it on a larger computer is substantial. Its main functions are to permit checks on the validity of the boundary conditions assumed for the small-area model described below and to allow detailed retrospective studies of particular surge episodes.

The governing equations used for the large-area model are based on those given by Proudman (Ref. 6), the only difference being the retention here of the nonlinear contribution of the surface elevation to the pressure gradient. The equations are:

$$\frac{\partial z}{\partial t} = - \frac{1}{a \cos\phi} \left[\frac{\partial}{\partial \phi} (U \cos\phi) + \frac{\partial V}{\partial \psi} \right] \qquad (1)$$

$$\frac{\partial U}{\partial t} = 2\omega \sin\phi \cdot V - \frac{g(h+z)}{a} \frac{\partial z}{\partial \phi} - \frac{h+z}{\rho a} \frac{\partial Pa}{\partial \phi} + \frac{1}{\rho} (F_s - F_b) \qquad (2)$$

$$\frac{\partial V}{\partial t} = - 2\omega \sin\phi \cdot U - \frac{g(h+z)}{a \cos\phi} \frac{\partial z}{\partial \psi} - \frac{h+z}{\rho a \cos\phi} \frac{\partial Pa}{\partial \psi} + \frac{1}{\rho} (G_s - G_b) \qquad (3)$$

where

t	=	time
ϕ, ψ	=	latitude and west-longitude respectively
z	=	elevation of sea surface
U, V	=	components of the volume transport
F_s, G_s	=	components of the tangential wind stress on the sea surface
F_B, G_B	=	components of bottom friction stress
Pa	=	atmospheric pressure on the sea
h	=	undisturbed water depth

BEAUFORT SEA LARGE-AREA MODEL

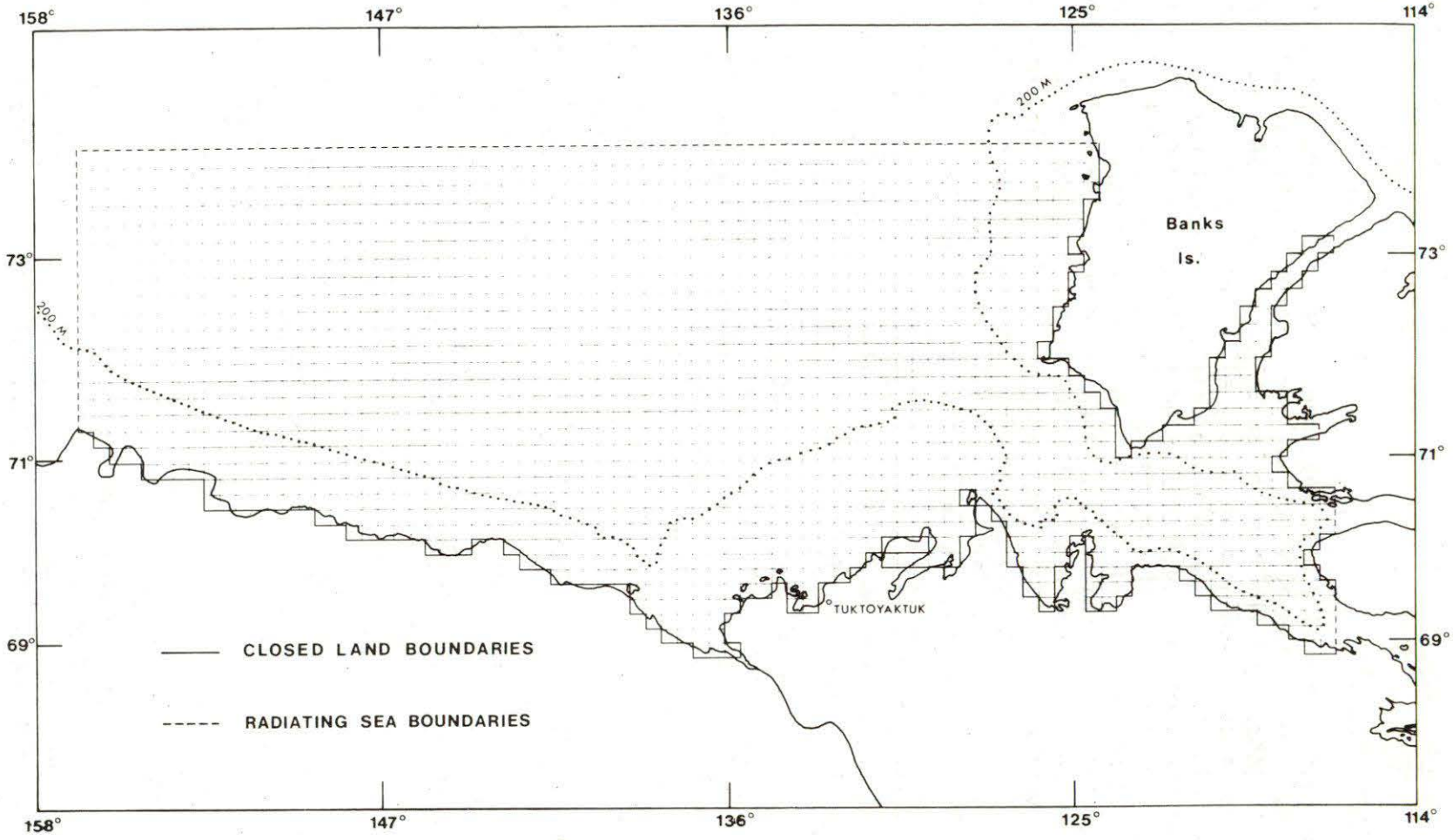

Figure 8

ρ = water density (assumed uniform and constant)
a = mean radius of the earth
g = acceleration due to gravity
ω = angular velocity of the earth.

Assuming quadratic friction laws, the bottom friction stress components are taken as

$$F_b = \frac{kU(U^2+V^2)^{\frac{1}{2}}}{(h+z)^2} \; ; \quad G_b = \frac{kV(U^2+V^2)^{\frac{1}{2}}}{(h+z)^2} \tag{4}$$

where k is a nondimensional bottom stress coefficient and the surface wind stresses F_s, G_s are the components in the ϕ, ψ directions respectively of the resultant wind stress

$$S = 1.25\ cR^2\ N/m^2 \tag{5}$$

where R is wind speed (m/s) and c is a nondimensional wind stress coefficient.

5.2 The Small-Area Model

This second model is designed to meet the need of the operational forecasting system for storm surge prediction with limited computing requirements. The necessary economies in computing time and memory are made by using a 30 km grid-length interval as opposed to the 18 km interval of the large-area model and by restricting the area modelled to the shallow Mackenzie-Bathurst shelf and its immediate environs. The coarser grid results in poorer fitting of the coastline but this is minimized by inclining the grid as shown in Figure 9. Since the use of inclined spherical polar coordinates involves much time-consuming evaluation of trigonometric functions, Cartesian coordinates were preferred. The inherent divergence error thus introduced is acceptable when the range of latitude is small, as in the present case.

The governing equations for the small-area model are

$$\frac{\partial z}{\partial t} = - \left[\frac{\partial U}{\partial x} + \frac{\partial V}{\partial y} \right] \tag{6}$$

$$\frac{\partial U}{\partial t} = 2\omega \sin\phi \; V - g(h+z) \frac{\partial z}{\partial x} - \frac{h+z}{\rho} \frac{\partial Pa}{\partial x} + \frac{1}{\rho} (F_s - F_b) \tag{7}$$

$$\frac{\partial V}{\partial t} = - 2\omega \sin\phi \; U - g(h+z) \frac{\partial z}{\partial y} - \frac{h+z}{\rho} \frac{\partial Pa}{\partial y} + \frac{1}{\rho} (G_s - G_b) \tag{8}$$

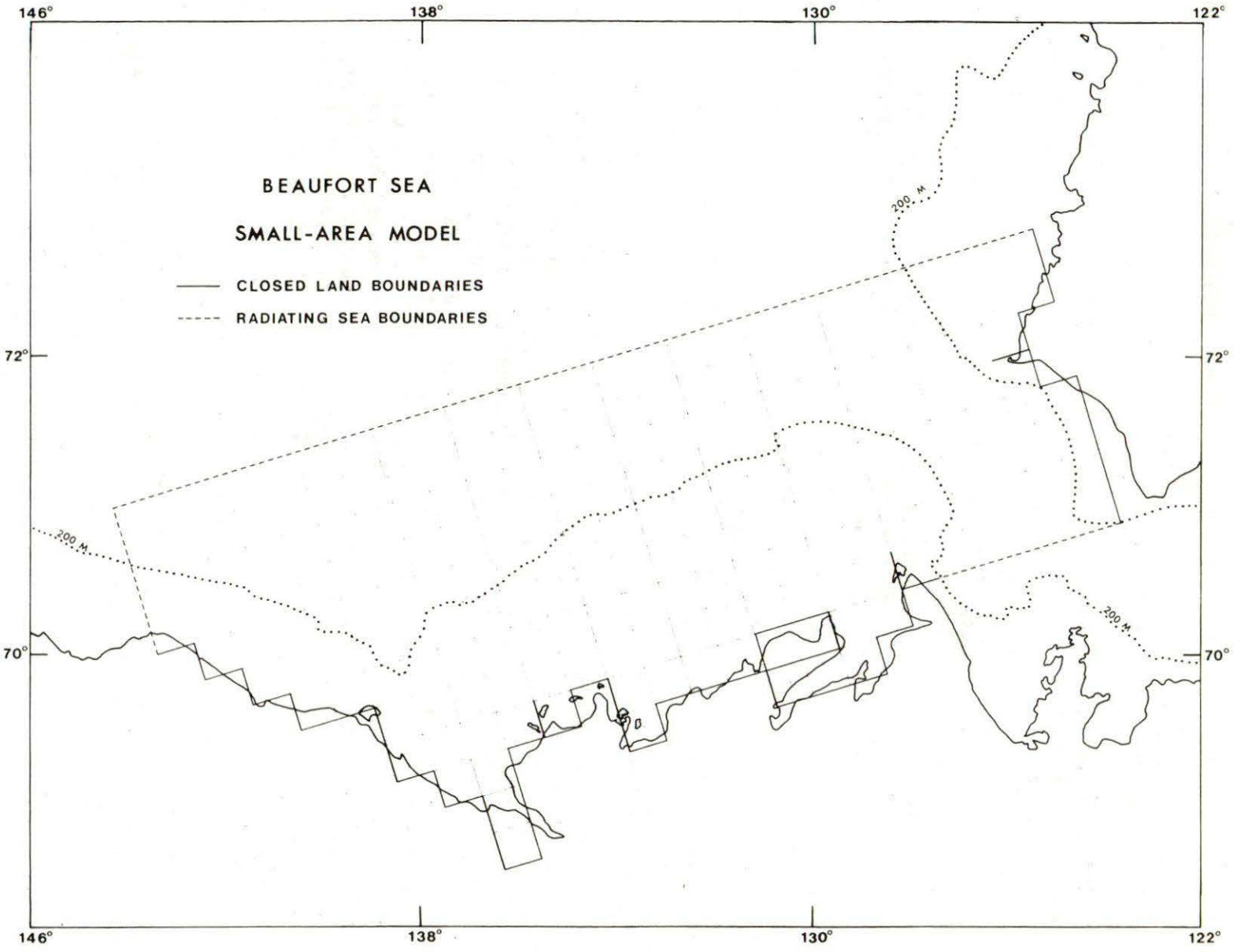
146°
138°
130°
122°
BEAUFORT SEA
SMALL-AREA MODEL
CLOSED LAND BOUNDARIES
RADIATING SEA BOUNDARIES
72°
70°
200 M
200 M
200 M

Figure 9

where

x,y	=	Cartesian coordinates aligned with the small-area model grid, i.e. pointing 17°W of N and 17°S of W (Fig. 9)
U,V	=	components of volume transport in the x,y directions
F_s,G_s	=	components of resultant wind stress, S, in the x,y directions
F_b,G_b	=	components of bottom friction stress in the x,y directions
ϕ	=	mean latitude of model

and the remaining notations have the same meanings as in equations (1) to (3). S, F_b and G_b are calculated using equations (5) and (4) as in the large-area model.

5.3 The Finite-Difference Scheme

The explicit difference scheme used to represent the governing partial differential equations was proposed originally by Sielecki (Ref. 7) and adapted by Heaps (Ref. 8) for storm surge simulation. For an interior point of the large-area model (Fig. 10), the sequence of computations followed in advancing from time $n.\Delta t$ to $(n+1).\Delta t$ is as follows:

$$z_{ij}^{n+1} = z_{ij}^{n} - \frac{\Delta t}{a \cos\phi_i}\left[\frac{U_{ij}^{n}\cos\bar{\phi}_i - U_{i-1,j}^{n}\cos\bar{\phi}_{i-1}}{\Delta\phi} + \frac{V_{i,j+1}^{n} - V_{ij}^{n}}{\Delta\psi}\right] \qquad (9)$$

$$U_{ij}^{n+1} = U_{ij}^{n} + \Delta t\left[2\omega \sin\bar{\phi}_i\, \tilde{V}_{ij}^{n} - \frac{g d_{ij}^{n+1}}{a}\,\frac{\{z_{i+1,j}^{n+1} - z_{ij}^{n+1}\}}{\Delta\phi} - \frac{d_{ij}^{n+1}}{\rho a}\left\{\frac{\partial Pa}{\partial\phi}\right\}_{ij}^{n+1} + \frac{1}{\rho}(F_s)_{ij}^{n+1} - \frac{k U_{ij}^{n+1}\{(U_{ij}^{n})^2 + (\tilde{V}_{ij}^{n})^2\}^{\frac{1}{2}}}{d_{ij}^{n}\, d_{ij}^{n+1}}\right] \qquad (10)$$

$$V_{ij}^{n+1} = V_{ij}^{n} + \Delta t\left[-2\omega \sin\phi_i\, \tilde{U}_{ij}^{n+1} - \frac{g D_{ij}^{n+1}}{a\cos\phi_i}\,\frac{\{z_{ij}^{n+1} - z_{ij-1}^{n+1}\}}{\Delta\psi} - \frac{D_{ij}^{n+1}}{\rho a \cos\phi_i}\left\{\frac{\partial Pa}{\partial\phi}\right\}_{ij}^{n+1} + \frac{1}{\rho}(G_s)_{ij}^{n+1} - \frac{k V_{ij}^{n+1}\{(\tilde{U}ij)^2 + (V_{ij}^{n})^2\}}{D_{ij}^{n}\, D_{ij}^{n+1}}\right] \qquad (11)$$

DETAILS OF LARGE-AREA MODEL GRID

Interior point

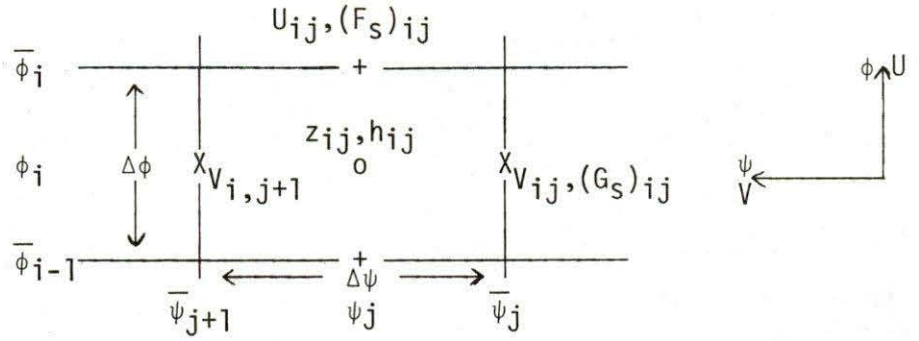

Closed Land Boundary

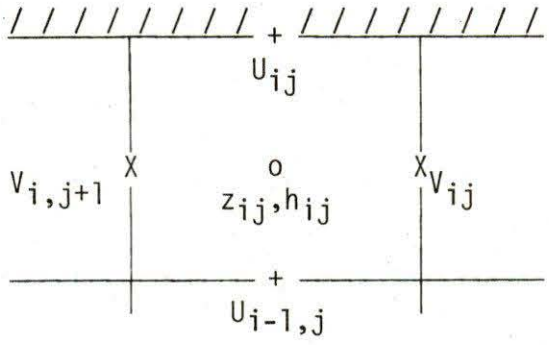

Boundary Condition:

$$U_{ij} \equiv 0$$

Radiating Sea Boundary

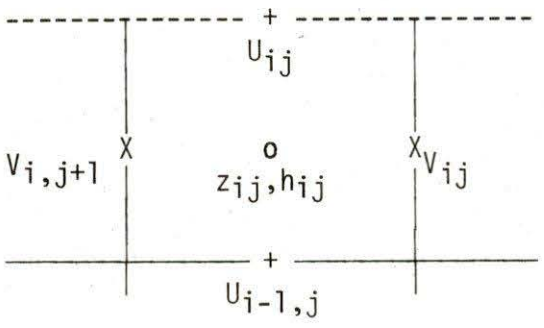

Boundary Condition:

$$U_{ij} = \{g[h_{ij} + z_{ij}]\}^{\frac{1}{2}} \cdot z_{ij}$$

Figure 10

The following terms in (9) to (11) are spatial averages formed at points where the required variable is not computed directly:

$$\tilde{U}^n_{ij} = \frac{1}{4}\left[U^n_{i-1,j-1} + U^n_{i,j-1} + U^n_{i-1,j} + U^n_{ij}\right]$$
$$\tilde{V}^{n+1}_{ij} = \frac{1}{4}\left[V^{n+1}_{i+1,j} + V^{n+1}_{i+1,j+1} + V^{n+1}_{ij} + V^{n+1}_{i,j+1}\right] \qquad (12)$$

Since it is convenient to store depth data only at z- points of the grid, the total water depths at U and V points respectively are represented by

$$d^n_{ij} = h_{ij} + \frac{1}{2}\left[z^n_{i,j} + z^n_{i+1,j}\right]$$
$$D^n_{ij} = h_{ij} + \frac{1}{2}\left[z^n_{i,j-1} + z^n_{i,j}\right] \qquad (13)$$

It will be noted that the old values of each of the variables z, U and V can be discarded in turn as the new values are calculated, thus economizing on storage requirements. Using basically the same difference scheme, the governing equations (6) to (8) of the small-area model are represented at each interior point (Fig. 11) by

$$z^{n+1}_{ij} = z^n_{ij} - \Delta t\left[\frac{U^n_{ij} - U^n_{i-1,j}}{\Delta x} + \frac{V^n_{i,j+1} - V^n_{ij}}{\Delta y}\right] \qquad (14)$$

$$U^{n+1}_{ij} = U^n_{ij} + \Delta t\left[\begin{array}{l} 2\omega\sin\phi\cdot\tilde{V}^n_{ij} - gd^{n+1}_{ij}\,\dfrac{\{z^{n+1}_{i+1,j} - z^n_{ij}\}}{\Delta x} \\ -\dfrac{d^n_{ij}}{\rho}\left(\dfrac{\partial Pa}{\partial x}\right)^{n+1}_{ij} + \dfrac{1}{\rho}(F_s)^{n+1}_{ij} - \dfrac{kU^{n+1}_{ij}\,\{(U^n_{ij})^2+(\tilde{V}^n_{ij})^2\}^{\frac{1}{2}}}{d^n_{ij}\cdot d^{n+1}_{ij}} \end{array}\right] \qquad (15)$$

$$V^{n+1}_{ij} = V^n_{ij} + \Delta t\left[\begin{array}{l} -2\omega\sin\phi\cdot\tilde{U}^{n+1}_{ij} - gD^n_{ij}\,\dfrac{\{z^{n+1}_{ij} - z^{n+1}_{i,j-1}\}}{\Delta y} \\ -\dfrac{D^n_{ij}}{\rho}\left(\dfrac{\partial Pa}{\partial x}\right)^{n+1}_{ij} + \dfrac{1}{\rho}(G_s)^{n+1}_{ij} - \dfrac{kV^{n+1}_{ij}\,\{(\tilde{U}_{ij})^2+(V^n_{ij})^2\}^{\frac{1}{2}}}{D^n_{ij}\cdot D^{n+1}_{ij}} \end{array}\right] \qquad (16)$$

DETAILS OF SMALL-AREA MODEL GRID

Interior point

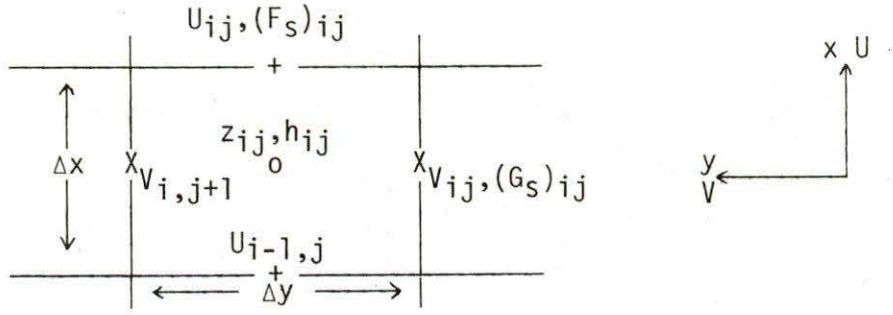

Closed Land Boundary

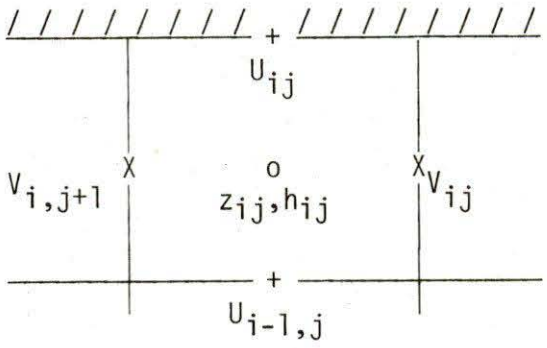

Boundary Condition:

$$U_{ij} \equiv 0$$

Radiating Sea Boundary

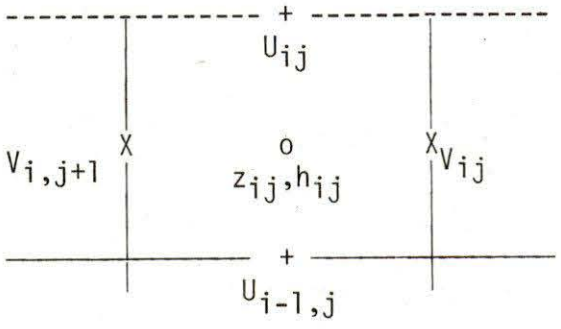

Boundary Condition:

$$U_{ij} = \{g[h_{ij} + z_{ij}]\}^{\frac{1}{2}} \cdot z_{ij}$$

Figure 11

where $\tilde{U}_{ij}$, $\tilde{V}_{ij}$, d^n_{ij}, D^n_{ij} are defined by (12) and (13). A relevant stability condition for this scheme is

$$\Delta t < \frac{\Delta x \cdot \Delta y}{\{gh_{max}\,(\Delta x^2 + \Delta y^2)\}^{\frac{1}{2}}} \qquad (17)$$

where h_{max} is the maximum depth over the model area. When Δy is chosen equal to Δx, (17) becomes

$$\Delta t < \frac{\Delta x}{(2gh_{max})^{\frac{1}{2}}} \qquad (18)$$

It will be noted that the atmospheric pressure gradient terms in equations (10), (11), (15) and (16) are not formed from differences of pressures at grid points of the oceanic models. The atmospheric pressure field is not usually known accurately enough for differentiation or differencing on this scale, and it is more satisfactory to calculate pressure gradients at the larger scales used for most meteorological charts and then obtain gradients at the model grid-points by interpolation among the smoother values thus obtained.

5.4 Boundary Conditions and Location

On account of computer capacity limitations, a model frequently has to be restricted to the area of direct interest, while other parts of the neighbouring seas with which the model area is continuous are simply omitted. Those parts of the grid boundary separating the area modelled from contiguous waters are generally known as open boundaries, though the term "sea boundaries" is preferred here. The problem of simulation of sea boundaries is not fully resolved, though there are several reasonably satisfactory methods in use for storm surge models. It has been observed that most surges are generated in shallow water and that contributions form neighbouring deep water are usually negligible. A common practice is to place the sea boundaries in deep water as far beyond the shallow area being modelled as computer memory limitations on grid size permit. The principal requirement on a sea boundary of this type is that it should appear 'open' to any component of the surge reaching the sea boundary, that is, a long wave approaching the sea boundary from the interior of the model should pass freely over the boundary and so disappear as though radiating out into a neighbouring deep semi-infinite ocean. The simplest technique used is to assume zero surface elevation at the open boundary, but this is the least satisfactory method, since this condition in fact produces perfect reflection. A better approximation to a fully open or radiating boundary, employed in Heaps (Ref. 16) and also in this study, is to assume all outward-travelling waves are normal to the boundary, and then by using the known relationship between volume transport and amplitude for a progressive wave,

to compute volume transport at the model boundary from the surface elevation at the nearest internal grid point. For instance, a wave travelling in the positive ϕ-direction in a system governed by equations (1) to (3) obeys the relation

$$U = \{gd\}^{\frac{1}{2}} z$$

where d is the local water depth. In this case, which is illustrated in Figure 10, this leads to the following difference form for the radiating boundary condition:

$$U_{i,j} = \{g(h_{ij} + z_{ij})\}^{\frac{1}{2}} z_{ij}$$

When a wave travelling in the negative ϕ-direction encounters a sea boundary, the boundary volume transport is given by

$$U_{i,j} = - \{g(h_{i+1,j} + z_{i+1,j})\}^{\frac{1}{2}} z_{i+1,j} .$$

Similarly, the radiation condition for a boundary at right angles to the ψ-direction is

$$V_{i,j} = \{g(h_{i,j-1} + z_{i,j-1})\}^{\frac{1}{2}} \cdot z_{i,j-1}$$

$$\text{or} \quad V_{i,j} = -\{g(h_{ij} + z_{ij})\}^{\frac{1}{2}} z_{ij}$$

depending on whether the wave approaching from the interior of the model is progressive or retrogressive.

Radiation conditions of the above type are used at all sea boundaries in the working versions of both the large-area and small-area models, though for comparison a test case, described in § 5.5, was run on the large-area model using the reflecting condition z = 0 on the sea boundary. The locations of the sea boundaries in the large-area model are well beyond the limits of the region in which surges are generated. In the small-area model, the sea boundaries were placed so that the abrupt edge of the shallow shelf lay a few grid-intervals inside the boundary (Fig. 9). A wave travelling outward over the shelf experiences reflection at the sudden change of depth and obeys the radiation condition at the sea boundary. There could be interference between the reflection and radiation processes if the radiating boundary ran too close to the edge of the shelf.

Since flooding of the coastal plain is not simulated in the existing models, representation of land boundaries is quite simple. The coast-

line is represented by the best possible continuous combination of grid segments parallel to the ϕ or ψ axes (x or y axes in the case of the small-area model) and zero normal transport is assumed, that is $U \equiv 0$ or $V \equiv 0$ respectively. An advantage of the difference scheme used here is that it permits representation of island chains or narrow peninsulas by putting $U \equiv 0$ or $V \equiv 0$ on appropriate grid-lines.

5.5 Surge Simulations

There are two aspects to model verification in the present study, only one of which can be examined adequately at the present time. First, there is the question of consistency between the two models. This can be checked just as well by simulating hypothetical storms as actual ones and thus there is no shortage of test cases. On the other hand, verifying that either model accurately duplicates real behaviour of the Beaufort Sea during actual surges cannot be fully checked in view of the shortage of suitable records, as discussed in § 4.2. For the sake of brevity, only simulations of the actual September 1972 surge will be discussed here, so that the questions of consistency and verisimilitude of the models can be discussed together.

Since knowledge of tidal patterns in the Beaufort Sea is far from complete, no attempt was made to simulate tides, and so, to permit comparison of simulated and observed records, the main diurnal and higher frequency tidal components were subtracted from the observed records. The resulting surge records for Atkinson Point and Cape Dalhousie are shown in Figure 12. At first, tangential wind stress and atmospheric pressure gradient inputs were used, but the effects of the latter were found to be very small for the 1972 surge and the runs discussed below were made with only wind stress as input. Figure 12 confirms that the barometric effect is negligible.

Figure 13 shows the results of one check made on the effects of the type of boundary chosen for the large-area model. The records shown are for shore points far from the boundary and for these it appears that it makes little difference which type of sea boundary is used. Similar tests showed that the same was true for all points on the shallow Mackenzie-Bathurst shelf and even some distance beyond the 200 m contour, and that it was only fairly close to the sea boundary that the choice of boundary condition became important.

Figures 14 and 15 show that the consistency of the large-area and small-area models is better at Atkinson Point and Cape Dalhousie than at Pelly Island and Cape Bathurst. This is probably due to the fact that the coastline at the latter is fitted only rather roughly by the coarser grid of the small-area model. At points even one or two grid intervals from the coast, there was very satisfactory consistency in elevations computed with the two models.

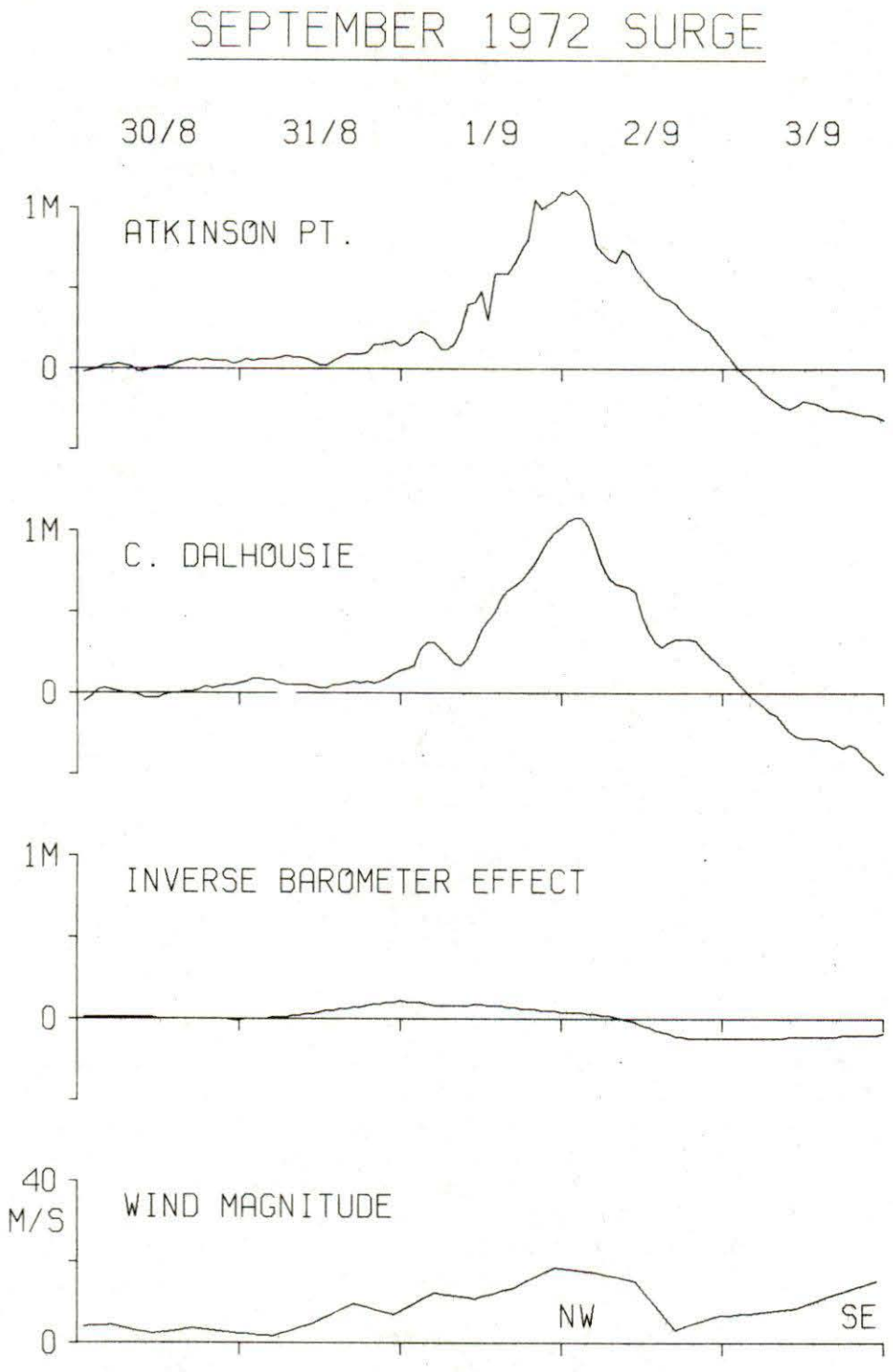

WATER LEVELS. INVERSE BAROMETER EFFECT AND GEOSTROPHIC WIND MAGNITUDE

Figure 12

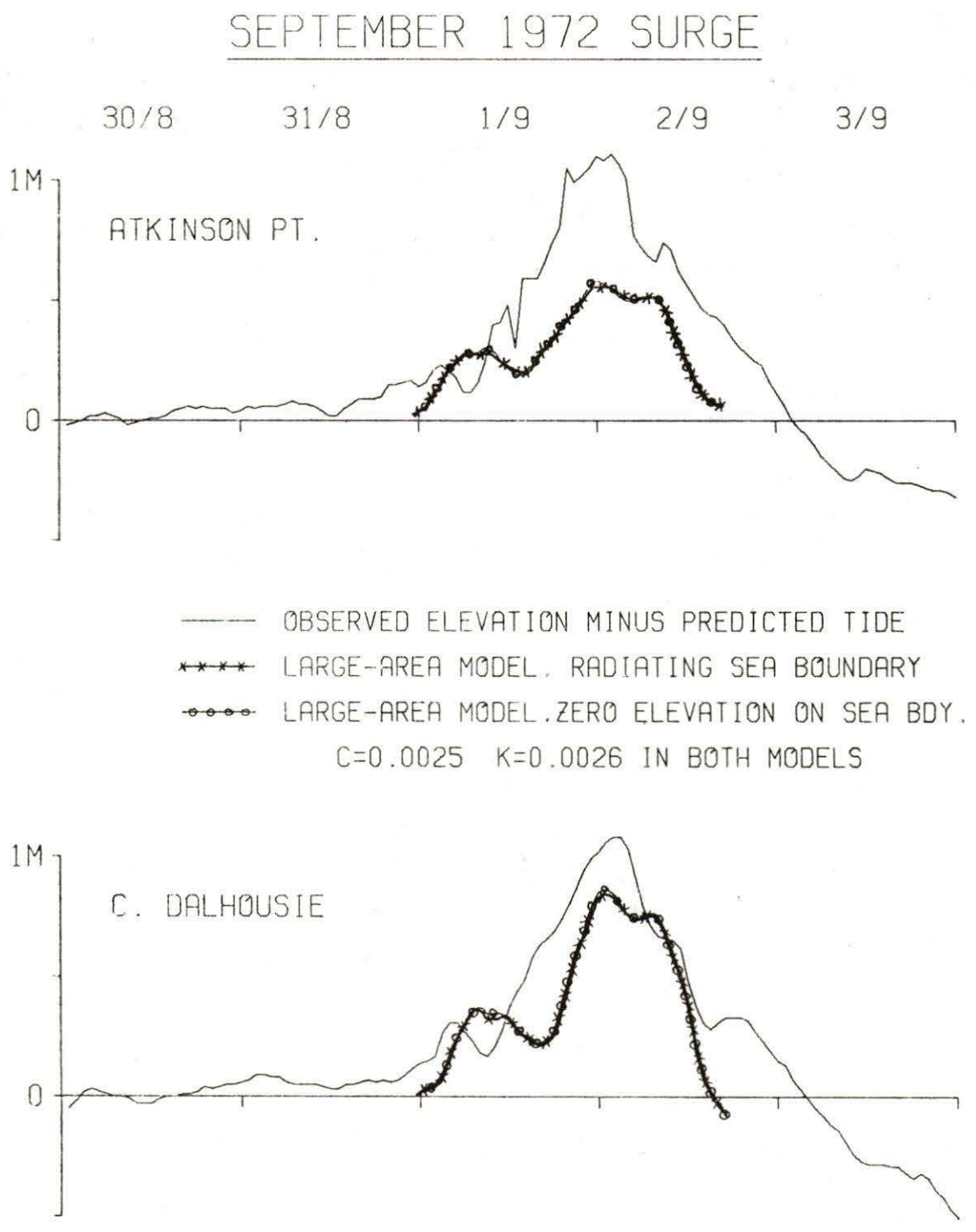
SEPTEMBER 1972 SURGE
30/8
31/8
1/9
2/9
3/9
1M
ATKINSON PT.
0
OBSERVED ELEVATION MINUS PREDICTED TIDE
LARGE-AREA MODEL. RADIATING SEA BOUNDARY
LARGE-AREA MODEL.ZERO ELEVATION ON SEA BDY.
C=0.0025 K=0.0026 IN BOTH MODELS
1M
C. DALHOUSIE
0
OBSERVED AND COMPUTED WATER LEVELS

Figure 13

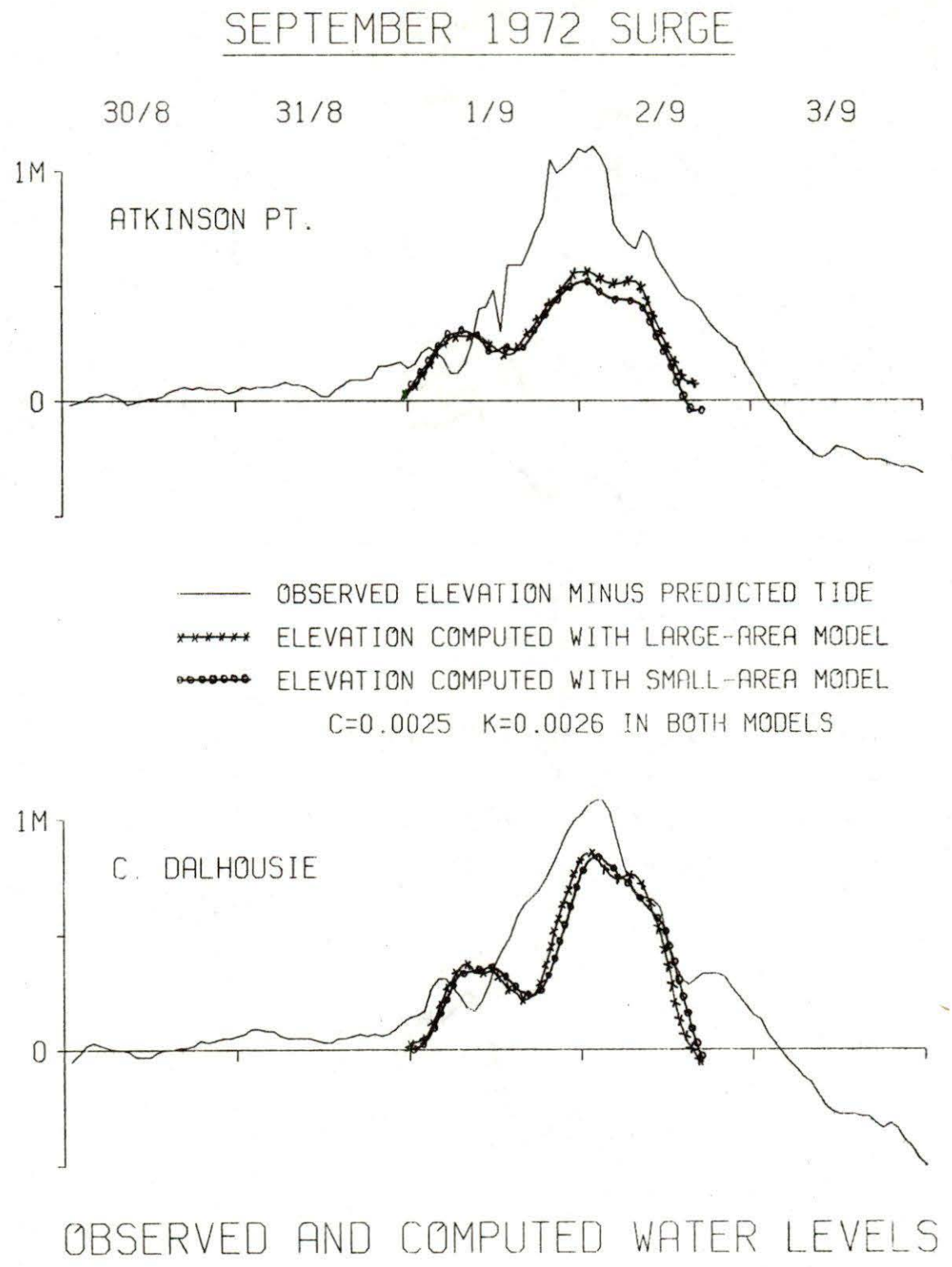
SEPTEMBER 1972 SURGE
30/8
31/8
1/9
2/9
3/9
1M
ATKINSON PT.
0
OBSERVED ELEVATION MINUS PREDICTED TIDE
ELEVATION COMPUTED WITH LARGE-AREA MODEL
ELEVATION COMPUTED WITH SMALL-AREA MODEL
C=0.0025 K=0.0026 IN BOTH MODELS
1M
C. DALHOUSIE
0
OBSERVED AND COMPUTED WATER LEVELS

Figure 14

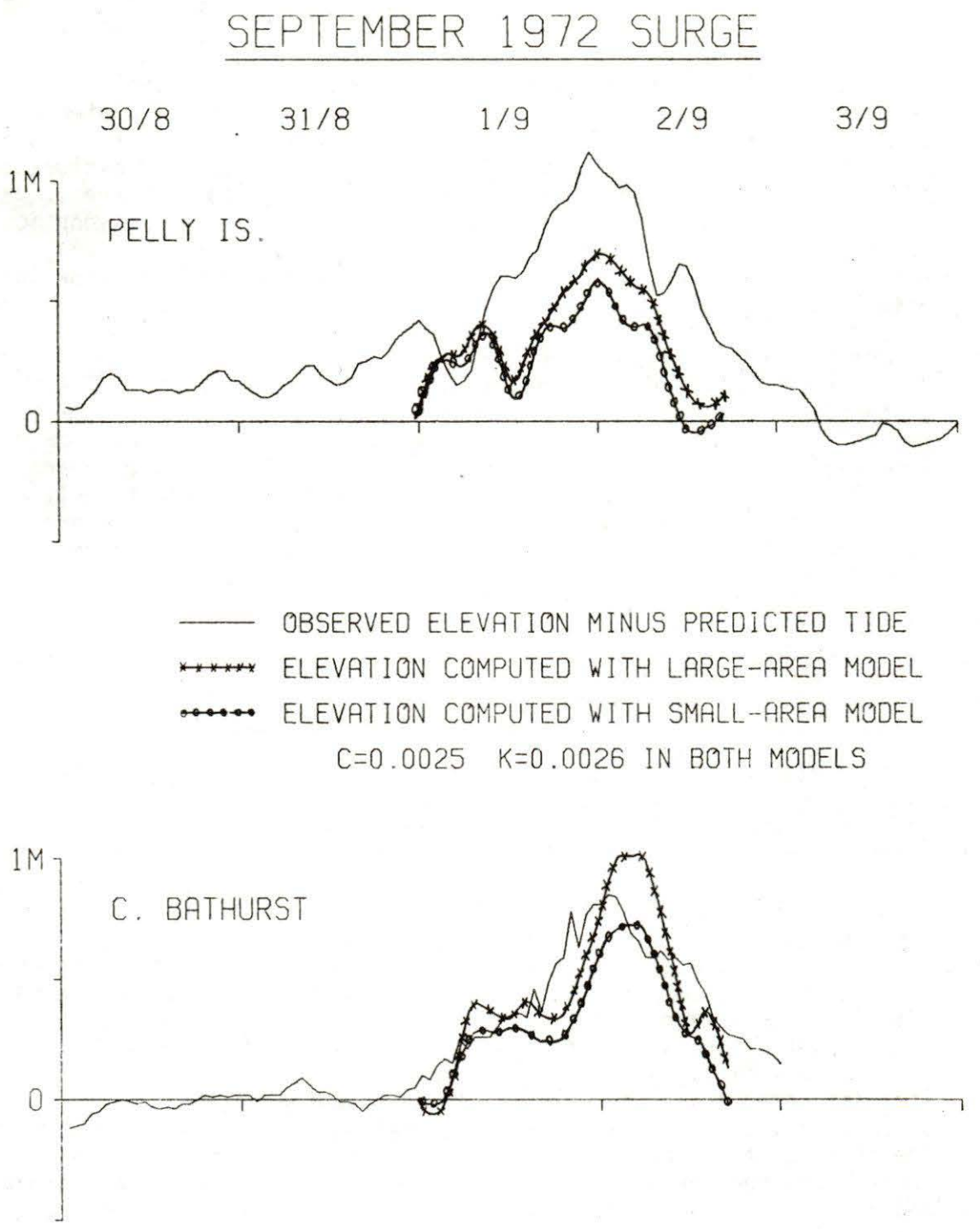
SEPTEMBER 1972 SURGE
30/8
31/8
1/9
2/9
3/9
1M
PELLY IS.
0
OBSERVED ELEVATION MINUS PREDICTED TIDE
ELEVATION COMPUTED WITH LARGE-AREA MODEL
ELEVATION COMPUTED WITH SMALL-AREA MODEL
C=0.0025 K=0.0026 IN BOTH MODELS
1M
C. BATHURST
0
OBSERVED AND COMPUTED WATER LEVELS

Figure 15

The discrepancies between the observed and simulated surges (Figures 14, 15) are substantial but are not disturbing, since the accuracy of the wind inputs is not high. Retrospective simulations of atmospheric behaviour during the September 1972 surge, using the meteorological models described later in § 6, are not yet available, so that the models had to be run using geostrophic winds calculated from measurements made from small-scale surface pressure charts such as Figure 4. Also, the scarcity of observations prevented exploration of which values of wind stress coefficient, c, and bottom stress coefficient, k, were best. For this purpose particularly, synoptic information is essential. The values $c = 0.0025$ and $k = 0.0026$ actually used are estimates, based on storm surge modelling experience elsewhere.

Figure 16 shows maximum surge levels reached on the Mackenzie-Bathurst shelf according to a simulation of the September 1972 surge on the large-area model. The amplifying effects of embayments are evident. Preliminary results from the 1975 records show maximum levels of 0.73 m, 0.30 m and 0.15 m at Atkinson Point, Site 13 and Site 5 respectively (see Figures 6 and 7) during the August 10/11 surge and maximum levels of 0.73 m, 0.40 m and 0.12 m at the same sites during the August 27 surge. These observations are in general accord with Figure 16, where it can be seen that maximum level attained decreases quickly with distance from the coast.

6. PROGNOSIS OF SURFACE WINDS

6.1 Simple Deduction of Surface Wind From Geostrophic Wind

Surface winds used for stress calculations in numerical storm surge models are usually obtained via estimates of geostrophic winds, which are in turn calculated from surface pressure gradients. The ratio of the observed surface wind, V_s, to the corresponding geostrophic wind, V_g, may happen to be reasonably constant for a particular region. Also, it may be possible to find a typical value for the 'cross-isobar angle', α, which expresses the difference in direction between the surface and geostrophic wind due to ground friction. Under light and moderate wind conditions there may be a fair amount of scatter in the estimates of V_s, V_g and α, due for instance to low-level instability, but such disturbing forces have less influence in the presence of large pressure gradients and consequently less variation from the mean values is likely during the intense storms conducive to storm surges. Once V_s, V_g and α are established for a region under study, prognosis of surface winds and consequent surge activity is possible if forecasts of surface pressure are available.

This simple method for predicting surface winds is not applicable to the Beaufort Sea for several reasons. In the first place, very few observations of surface winds at sea have been made, as shipping in the area is sparse and limited to the summer months. Figure 17 shows V_s, V_g and α calculated for observations made in the summer of 1974 by the research vessel M.V. *THETA* in Mackenzie Bay. The degree

SEPTEMBER 1972 SURGE SIMULATION
MAXIMUM ELEVATION (M)

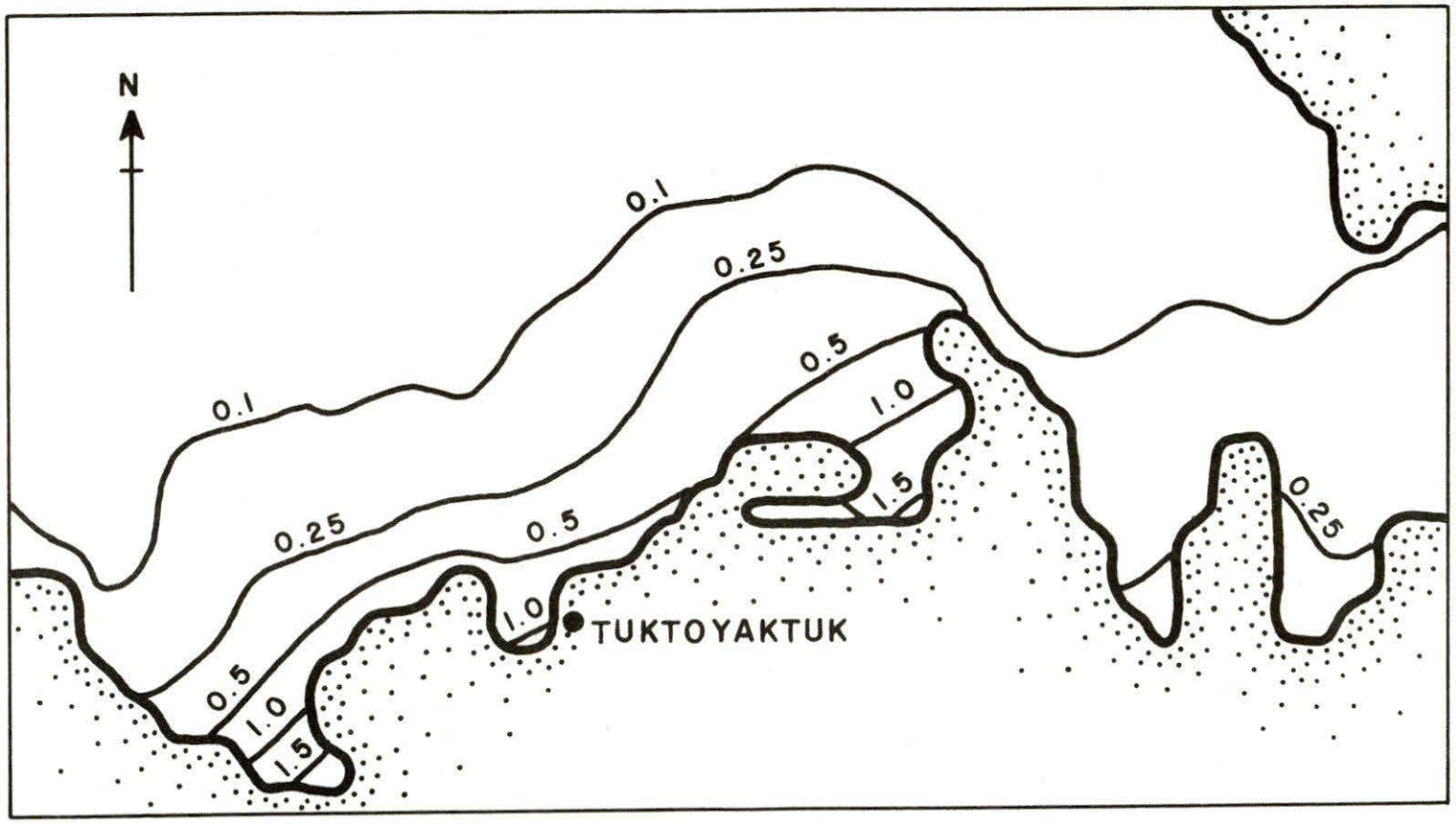

Figure 16

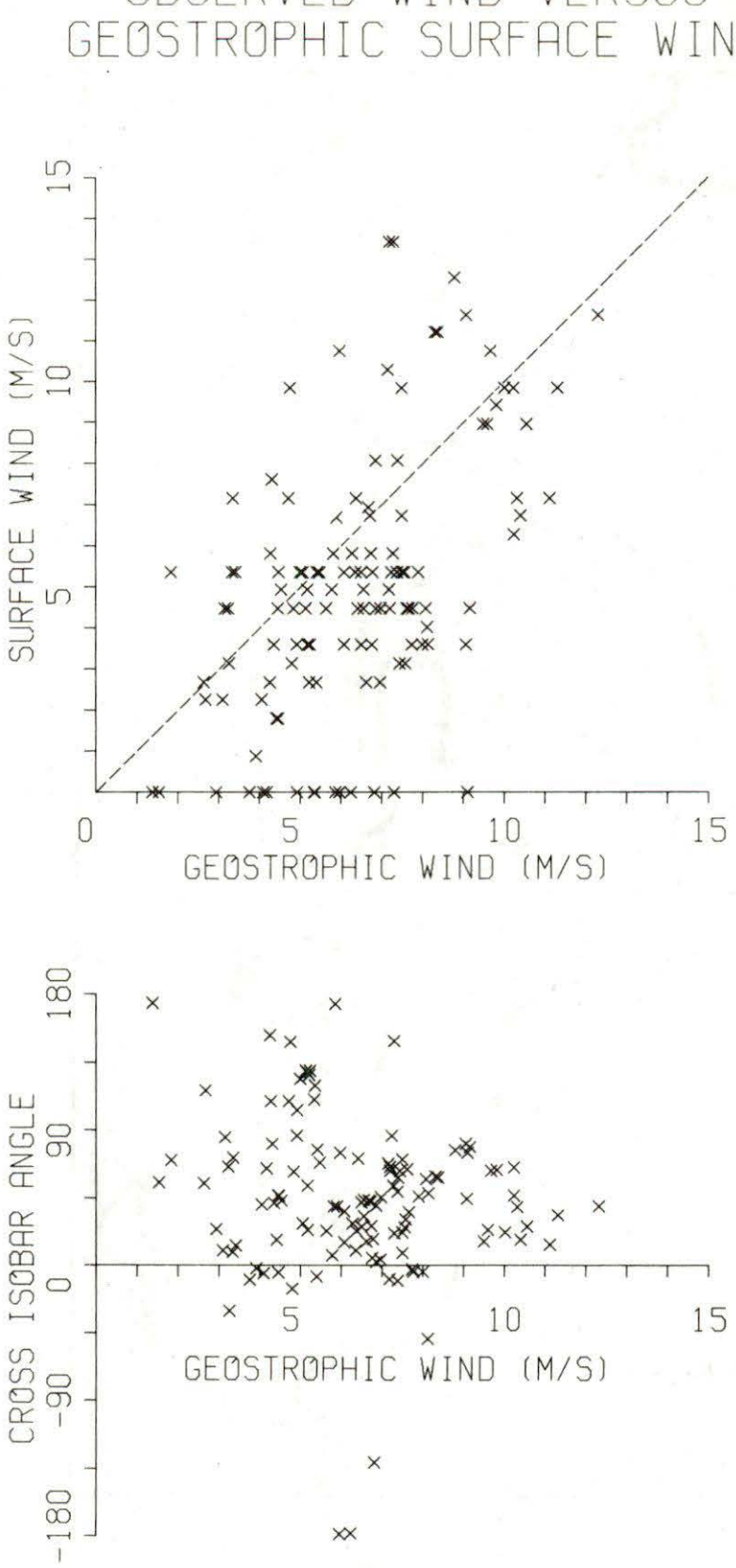
OBSERVED WIND VERSUS
GEOSTROPHIC SURFACE WIND
SURFACE WIND (M/S)
0
5
10
15
GEOSTROPHIC WIND (M/S)
CROSS ISOBAR ANGLE
180
90
0
-90
-180
5
10
15
GEOSTROPHIC WIND (M/S)

Figure 17

of scatter is very marked and no episodes of winds high enough to cause surges were recorded. Secondly, observations of surface winds would be required over several years to determine how V_s,V_g and α vary with the proportion of ice cover. Use of values established for other geographic regions is inadvisable, since both V_s/V_g and α may vary with latitude (Ref. 9). Values calculated from observations at shore stations are also unsuitable, since these are influenced by local topography, and in addition surface friction is greater over land.

6.2 Surface Wind From Numerical Meteorological Models

As part of the Beaufort Sea Project, several more sophisticated approaches to the problem of predicting surface winds or surface wind stress are in progress, using numerical models. On the largest scale and underlying the other modelling efforts, is an operational 5-level primitive equation model of the northern hemisphere developed at the Canadian Meteorological Centre, Montreal. This predicts pressures and other variables at 6-hour intervals up to 36 hours ahead; runs are initiated with new input data every 12 hours. At present a grid length of 381 km (at 60°N) is used and surface topography can be described only in highly-smoothed form. Physical effects included are heating from the underlying surface, convective adjustment, horizontal diffusion of all variables and vertical diffusion of all variables except temperature. It is anticipated that by 1976 the grid length will have been reduced to 190 km or less and a few more physical effects included. Forecasts will be initiated at 6-hour rather than 12-hour intervals and will be continued out to 60 hours. These improvements together with the proposed deployment of automated weather stations on the Beaufort Sea pack ice to provide better synoptic surface data input, should ensure fairly accurate large-scale wind forecasts.

Regional improvement of the CMC forecasts is obtained by use of a two-level vorticity model, known as RUM (for Regional Update Model) developed by Atmospheric Environment Service, Toronto (Ref. 10). RUM obtains initial and boundary conditions by temporal and spatial interpolation of the CMC 500 mb forecasts and then uses more recent surface pressure observations to obtain improved estimates of the surface pressure field and geostrophic wind. Given the latter and surface temperature information from which to determine the low-level stability, surface winds are computed using a Rusinger-type boundary layer (Ref. 11). RUM is designed to run economically on small computers in regional weather offices and can be re-initiated whenever new surface data is acquired. The RUM grid interval of 127 km permits somewhat better orographic description than the CMC model. The present version does not include simulation of heating and friction, but it is intended to include these later. Tests made in other areas show that even in its present form, RUM does provide improved forecasts, in the short run at least (Ref. 12). The RUM developed for the Beaufort Sea is now operational at Arctic Weather Central, Edmonton, and comparison of forecast and observed surface conditions over the summer of 1975 will indicate for how many hours RUM forecasts offer an improvement over those of

the CMC model at each phase of the 12-hour CMC forecast style. Smooth change-over from one forecast model to the other can be accomplished easily by using a weighted sum of both forecasts at all times and varying the weighting coefficients as forecast time increases.

Although both RUM and the CMC model can provide surface wind forecasts, neither has a grid-scale small enough to cope adequately with the horizontal variation of wind over the southern Beaufort Sea. For this reason it is planned to incorporate a third model into the forecasting system. This is a mesoscale one-level primitive equation boundary layer model, developed by Danard (Ref. 13) which has already been tested in other areas, with grid lengths of 5 to 20 km. Given a large-scale diagnosis or prognosis of the sea-level pressure field from either RUM or the CMC model, this model modifies the pressure field to account for mesoscale influences. For instance, surface pressure is raised over ice or cold water and lowered over warm water. Effects such as frictional mass convergence, differential heating between ice, land and water and orographic channelling are included, as are differences in friction between ice, land and water. Then the surface wind and stress are calculated from the modified pressure field taking into account atmospheric stability in a manner adopted from Deardorff (Ref. 14).

To permit calibration of the storm surge models, retrospective simulations of wind behaviour during major surge episodes such as that of September 1972 are being carried out using the three models described above and also on an independent 8-level 95 km grid-length primitive equation model (Ref. 15) which simulates some physical processes not yet included in the other models, for instance sub-grid scale precipitation. Computer time limitations do not permit this last model to be run operationally as part of the Beaufort Sea forecasting system.

At the present time, only historical data on sea-surface temperature is available for use in estimating low-level stability, but it is expected that before long processing of surface data from satellites can be speeded up to a point where practically current surface temperature data can be made available.

7. NEGATIVE SURGES AND WINTER SURGES

7.1 Negative Surges

Temporary decreases in sea-level of about 1 m can occur at Tuktoyaktuk (Figure 3) in response to strong off-shore winds. These *negative surges* could obviously hinder, if not endanger, the largest vessels which might use the harbour, as the normal draft in the approaches is only 4 m. The numerical models developed for positive surges can be used equally well to simulate negative surges, as tangential wind stress on the sea surface is the driving mechanism in both cases, and predictions of abnormally low water levels in the approaches to Tuktoyaktuk could be given some hours in advance.

7.2 Winter Surges

No winter surges were recorded at Tuktoyaktuk in the first eleven years following the installation of a tide gauge in 1962. Since records are about 90% complete, it can be concluded that positive winter surges are rare or at least unusual. Nevertheless, in the 1973-74 winter, two surges of about 1 m were observed. While these are not large by summer surge standards (see for instance Figure 3), it must be remembered that even moderately high water levels in winter can result in large ice masses being pushed up the beaches and that substantial damage could ensue to shore installations placed too close to the waterline.

The first of these winter surges was caused by an intense low which passed eastwards above the latitude of Banks Island during 10-15 November, 1973. The surface pressure chart in Figure 18 shows the peak of the storm. Winds over the Mackenzie-Bathurst shelf were almost due west throughout. Figure 19 shows water levels (minus predicted tide) at the three gauges operating at that time (Figure 6). A noteworthy feature of this surge is the long delay between the occurrence of peak wind speed and maximum surge height. A possible explanation is that in view of the wind direction, the water was initially set in motion eastwards and was then diverted towards the coast by Coriolis effect, which requires some time to have an appreciable result. It will also be remarked that peak wind velocity was nearly double that of the September 1972 surge, which, if the quadratic stress law holds, implies quadrupled tangential wind stress, yet the elevations reached during the two surges were comparable. It must be concluded that the effectiveness with which wind can generate a surge is greatly reduced when there is fairly complete ice cover, as there was in November 1973.

Figure 20 shows surface pressures during the peak of the storm which produced the surge of 5-7 January, 1974 (Figure 21). Again the elevations reached are less than would be expected with the same wind under ice-free conditions. A most interesting feature of this surge is that the water levels reached a maximum on January 6 and then began to decrease, although the wind intensity remained high until 7 January. Possibly this indicates that at first a certain amount of movement was possible in the ice cover, due to the presence of leads, and this permitted the transmission of tangential stress to the water, but that by January 6 all the slack in the ice cover had been taken up and stress could no longer be transmitted to sustain the surge.

A notable feature of both winter surges is that the maximum elevations measured at the off-shore site are much closer in magnitude to the elevations at the shore than is the case with summer surges (§ 5.5). This may be due to landfast ice sheltering the zone of shallowest water close to shore, where a substantial portion of any summer surge would be generated.

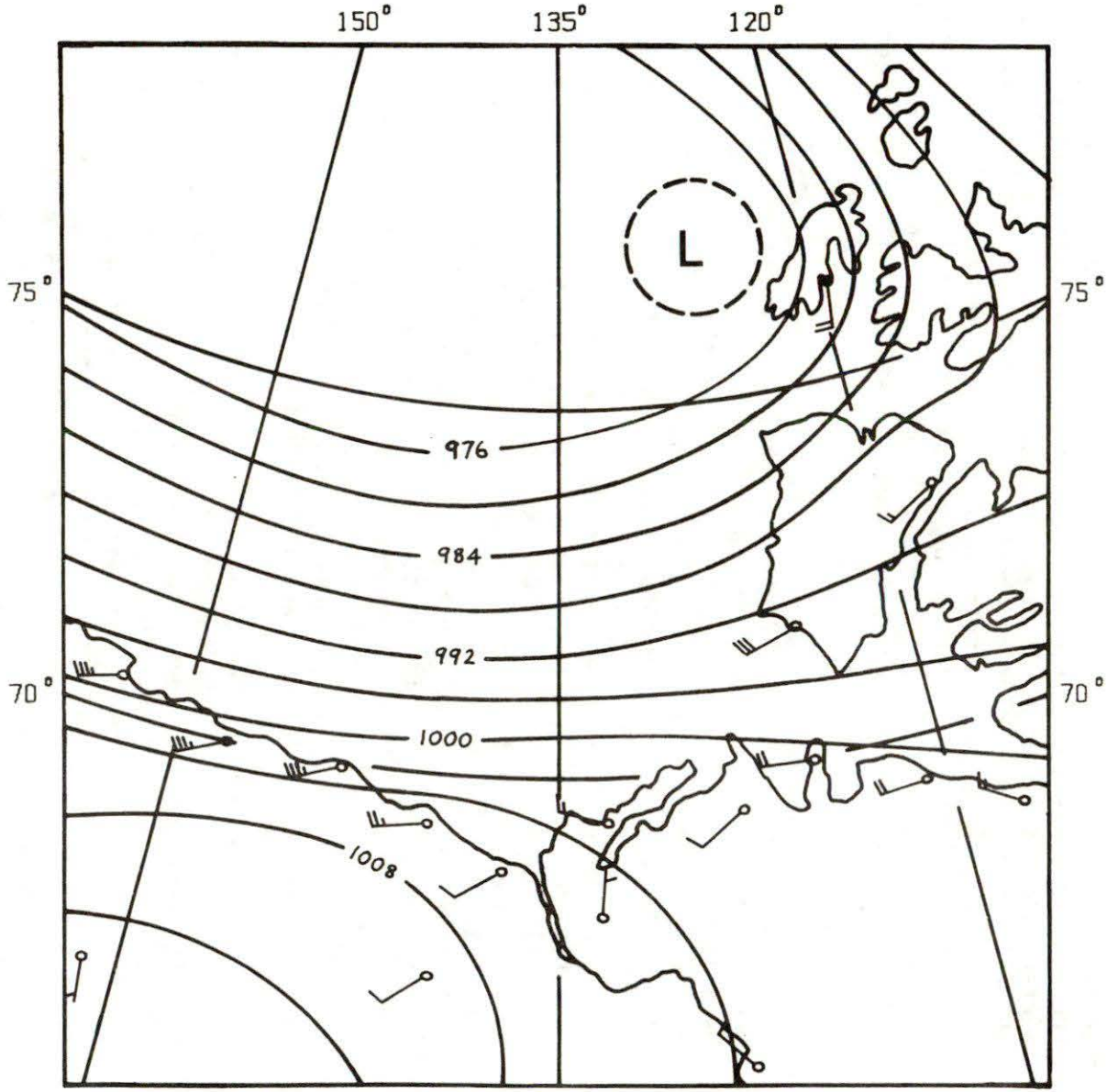
150°
135°
120°
75°
75°
70°
70°
L
976
984
992
1000
1008
SURFACE PRESSURE (MB) AT 0000 GMT 12 NOV 1973

Figure 18

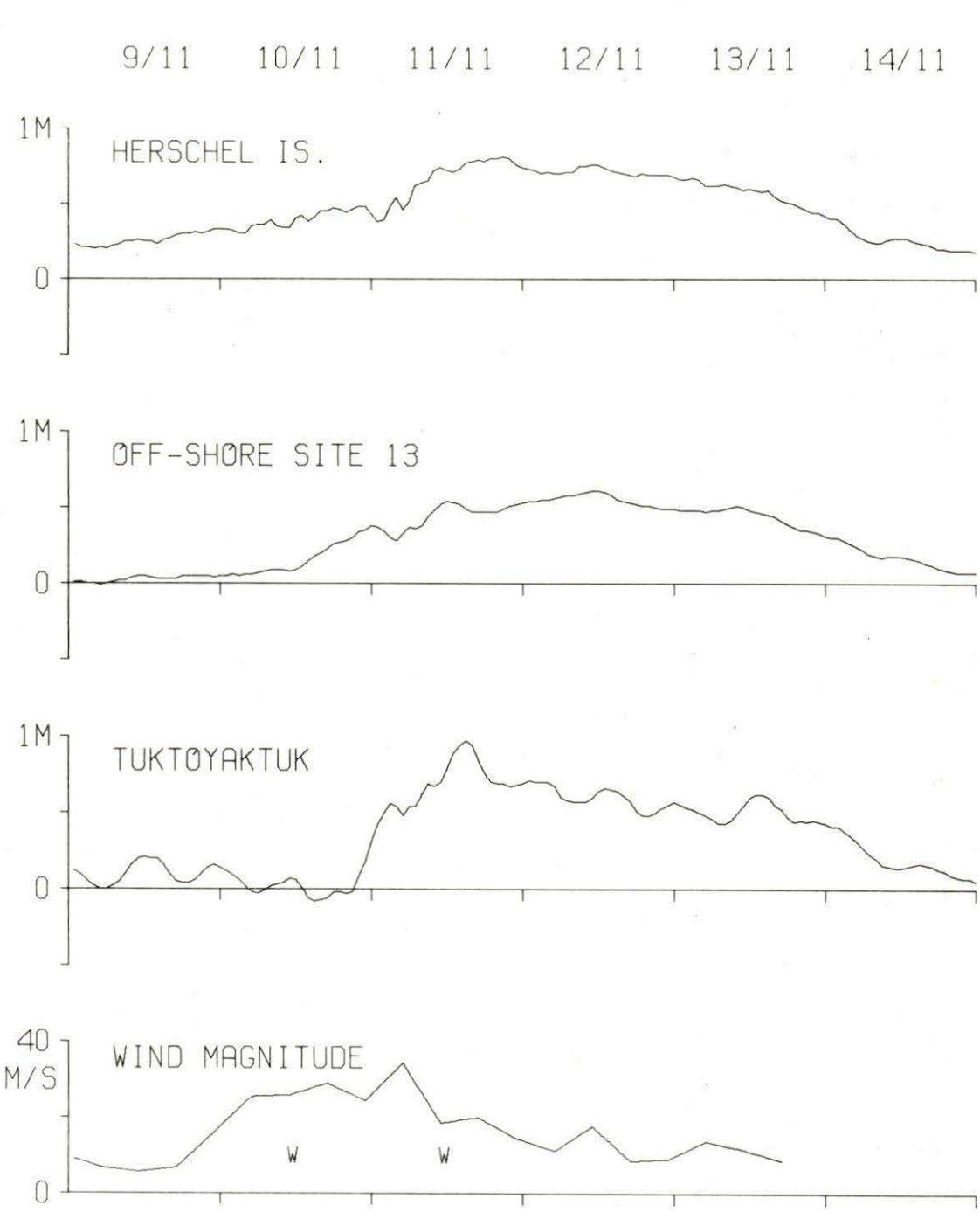

WATER LEVELS AND GEOSTROPHIC WIND MAGNITUDE

Figure 19

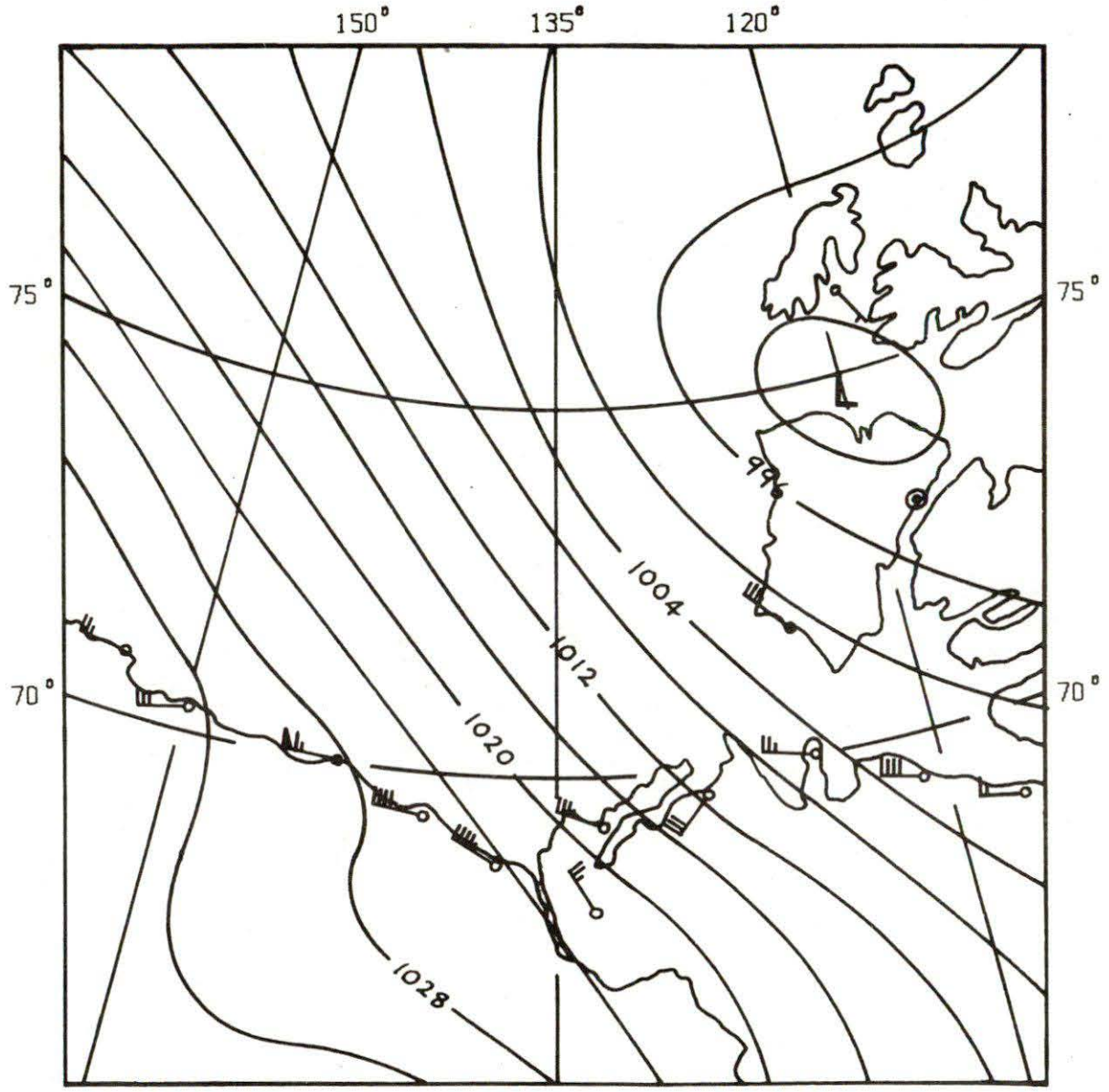
150°
135°
120°
75°
75°
70°
70°
L
992
1004
1012
1020
1028
SURFACE PRESSURE (MB) AT 1200 GMT 6 JAN 1974

Figure 20

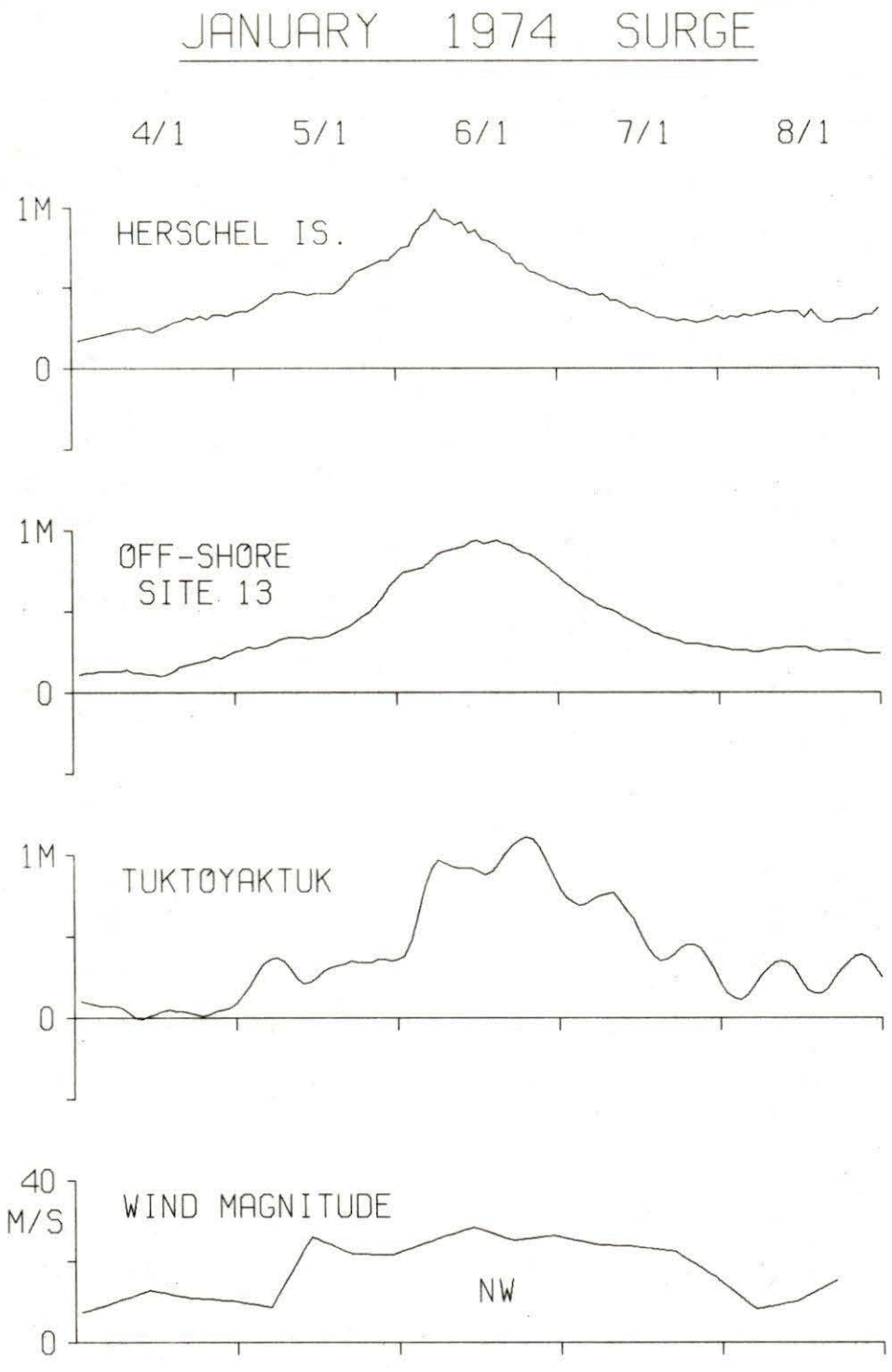

WATER LEVELS AND GEOSTROPHIC WIND MAGNITUDE

Figure 21

8. CONCLUSIONS AND RECOMMENDATIONS

Storm surges are a significant feature of the physical oceanography of the southern Beaufort Sea, especially in good ice years, but their amplitudes at sites well off-shore are probably too small to pose any hazard to drilling operations. Installations near shore should be designed to cope during storms with water levels at least 2 m above normal, with additional allowance for short period wind waves (see Beaufort Sea Technical Report No. 21).

Consideration should be given to large-scale cleanup operations on the low-lying nesting grounds near the coast. The existence of the bird population proves its ability to survive occasional flooding by water alone, but cleanup of a large area before the next breeding season would probably be essential if oil was also carried inland during a surge.

The numerical models developed for retrospective and predictive simulations of Beaufort Sea storm surges cannot be fully verified, that is, quantitatively checked and tuned, until several more surges are recorded, a process which may require a network of tide gauges to be deployed for several years. Since synoptic coverage is important, regular operation of water level recorders at all oil exploration sites would be a most valuable supplement to future field programs. Similarly, regular meteorological observations at sea would be very valuable for checking out the meteorological models on whose accuracy the storm surge predictions largely depend.

9. ACKNOWLEDGEMENTS

The writer wishes to thank Dr. N.S. Heaps, for designing the large-area model and for many useful discussions, Dr. M.B. Danard for much information on meteorological models, Mr. M.G. Foreman, for programming the numerical models, Mrs. C. Wallace for assisting in preparation of the diagrams and Mrs. Anne Nichol and Mrs. Lynne Egan for typing the report. Thanks are also due to many other people engaged in the Beaufort Sea Project, in particular, personnel of the Atmospheric Environment Service and the Canadian Hydrographic Service for their extensive cooperation.

10. REFERENCES

1. B.C. McDonald and C.P. Lewis, 1973, "Geomorphic and Sedimentologic Processes of Rivers and Coast, Yukon Coastal Plain", Task Force on Northern Oil Development, Report No. 73-39, Information Canada.

2. D. A. Healey, 1971, "Oceanographic Observations in the Beaufort Sea, July 15-September 4, 1970", Pacific Marine Science Report 71-3, Marine Sciences Branch, Department of Fisheries and Forestry, Victoria, B.C. (Unpublished Manuscript).

3. R.H. Herlinveaux and B. de Lange Boom, 1974, "Physical Oceanography in the Southern Beaufort Sea", Interim Report D-4, Beaufort Sea Project, Environment Canada, Victoria, B.C.

4. B.M. Burns, 1973, "The Climate of the Mackenzie Valley-Beaufort Sea", 2 vols., Climatological Studies, No. 24, Atmospheric Environment Service, Toronto.

5. Anon., 1971, "Beaufort Sea Storm, September 13-16, 1970, Investigation of Effects in the Mackenzie Delta Region", Engineering Programs Branch, Department of Public Works, Ottawa.

6. J. Proudman, 1954, "Note on the Dynamics of Storm Surges", Mon. Nat. R. Astr. Soc., Geophys. Suppl., Vol. 7, pp 44-48.

7. A. Sielecki, 1968, "An Energy-Conserving Difference Scheme for the Storm Surge Equations", Mon. Wea. Rev., Vol. 96, pp 150-156.

8. R. A. Flather and N.S. Heaps, 1975, "Tidal Computations for Morecambe Bay", Geophys. J.R. Astr. Soc., Vol. 42, pp 489-518.

9. L.P. Carstensen, 1967, "Some Effects of Sea-Air Temperature, Latitude and Other Factors on Surface Wind-Geostrophic Wind Ratio and Deflection Angle", Technical Report No. 29, Fleet Numerical Weather Facility, Monterey.

10. F.J. Winninghoff, 1973, "On Regional Update Modelling", Unpublished Report, Forecast Research Division, Atmospheric Environment Service, Toronto.

11. J.A. Businger, J.C. Wyngaard, Y. Izumi and E.F. Bradley, 1971, "Flux-Profile Relationships in the Atmospheric Surface Layer", J. Atmos. Sci., Vol. 28, No. 2, pp 181-189.

12. E.C. Jarvis, 1975, "Report on the Performance of Regional Update Models", Unpublished Report, Forecast Research Division, Atmospheric Environment Service, Toronto.

13. M.B. Danard, 1973, "A Simple Model for Orographic Influences on Surface Winds", Proc. Third Int. Clean Air Congress, Dusseldorf, Oct. 8-12, 1973. (in press)

14. J.W. Deardorff, 1972, "Parameterization of the Planetary Boundary Layer for Use in General Circulation Models", Mon. Wea. Rev., Vol. 100, pp 93-106.

15. V.R. Neralla and M.B. Danard, 1975, "Incorporation of Parameterized Convection in the Synoptic Study of Large Scale Effects of the Great Lakes", Mon. Wea. Rev., Vol. 103, pp 388-405.

16. N.S. Heaps, 1974, "Development of a Three-Dimensional Numerical Model of the Irish Sea", Rapp. P.-v Réun. Cons. int. Explor. Mer, Vol. 167, pp 147-162.